Since January 2020 Elsevier has created a COVID-19 resource centre with free information in English and Mandarin on the novel coronavirus COVID-19. The COVID-19 resource centre is hosted on Elsevier Connect, the company's public news and information website.

Cell Reports

Article

BNT162b2-induced neutralizing and non-neutralizing antibody functions against SARS-CoV-2 diminish with age

Graphical abstract

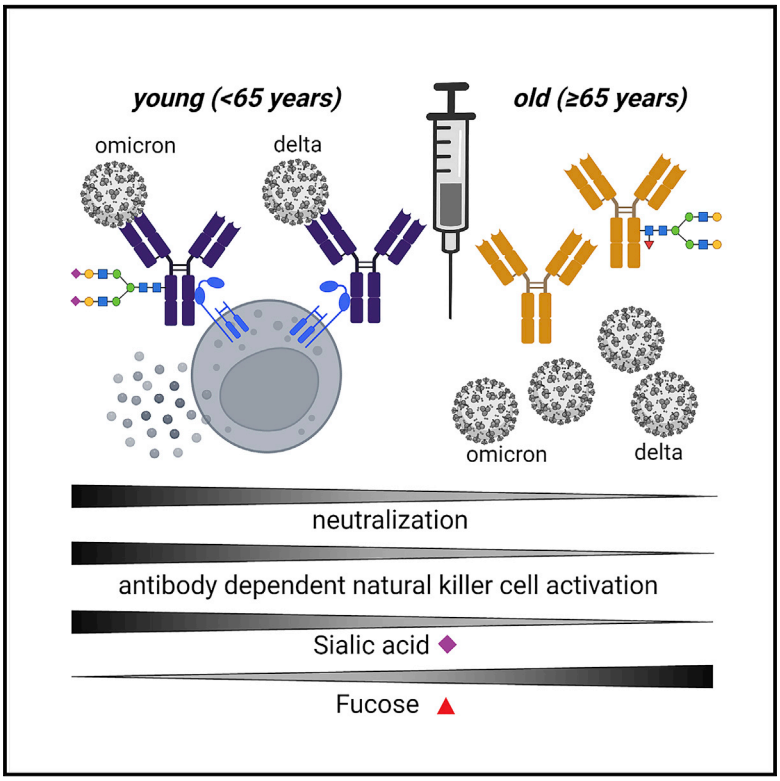

Highlights

- Vaccination induces neutralization and Fc effector functions against SARS-CoV-2
- Vaccine-induced FcγRIIIa/CD16a effector functions correlate with neutralization
- Vaccine-specific IgG afucosylation and sialylation link to CD16a effector functions
- Age influences vaccine-induced polyfunctional antibody breadth and magnitude

Authors

Timothy A. Bates, Pei Lu, Ye Jin Kang, ..., Marcel E. Curlin, Fikadu G. Tafesse, Lenette L. Lu

Correspondence

curlin@ohsu.edu (M.E.C.), tafesse@ohsu.edu (F.G.T.), lenette.lu@utsouthwestern.edu (L.L.L.)

In brief

Bates et al. investigate viral neutralization, antibody glycosylation, and Fc-mediated effector functions from BNT162b2. Neutralization and antibody-dependent natural killer cell activation correlate. Vaccine-specific IgG display distinct glycosylation patterns with afucosylation and sialylation associating with natural killer cell activation. These antibody properties collectively diminish in those ≥65 years old.

Bates et al., 2022, Cell Reports *41*, 111544
October 25, 2022
https://doi.org/10.1016/j.celrep.2022.111544

CellPress

Cell Reports

CellPress
OPEN ACCESS

Article

BNT162b2-induced neutralizing and non-neutralizing antibody functions against SARS-CoV-2 diminish with age

Timothy A. Bates,[1,7] Pei Lu,[2,7] Ye Jin Kang,[2] Devin Schoen,[3] Micah Thornton,[4] Savannah K. McBride,[1] Chanhee Park,[4] Daehwan Kim,[4] William B. Messer,[1] Marcel E. Curlin,[3,*] Fikadu G. Tafesse,[1,*] and Lenette L. Lu[2,5,6,8,*]

[1]Department of Molecular Microbiology and Immunology, Oregon Health and Sciences University, Portland, OR 97239, USA
[2]Division of Infectious Diseases and Geographic Medicine, Department of Internal Medicine, UT Southwestern Medical Center, Dallas, TX 75390, USA
[3]Department of Occupational Health, Oregon Health and Sciences University, Portland, OR 97239, USA
[4]Lyda Hill Department of Bioinformatics, UT Southwestern Medical Center, Dallas, TX 75390, USA
[5]Department of Immunology, UT Southwestern Medical Center, Dallas, TX 75390, USA
[6]Parkland Health & Hospital System, Dallas, TX 75235, USA
[7]These authors contributed equally
[8]Lead contact
*Correspondence: curlin@ohsu.edu (M.E.C.), tafesse@ohsu.edu (F.G.T.), lenette.lu@utsouthwestern.edu (L.L.L.)
https://doi.org/10.1016/j.celrep.2022.111544

SUMMARY

Each severe acute respiratory syndrome coronavirus 2 (SARS-CoV-2) variant renews concerns about decreased vaccine neutralization weakening efficacy. However, while prevention of infection varies, protection from disease remains and implicates immunity beyond neutralization in vaccine efficacy. Polyclonal antibodies function through Fab domains that neutralize virus and Fc domains that induce non-neutralizing responses via engagement of Fc receptors on immune cells. To understand how vaccines promote protection, we leverage sera from 51 SARS-CoV-2 uninfected individuals after two doses of the BNT162b2 mRNA vaccine. We show that neutralizing activities against clinical isolates of wild-type and five SARS-CoV-2 variants, including Omicron BA.2, link to FcγRIIIa/CD16 non-neutralizing effector functions. This is associated with post-translational afucosylation and sialylation of vaccine-specific antibodies. Further, polyfunctional neutralizing and non-neutralizing breadth, magnitude, and coordination diminish with age. Thus, studying Fc functions in addition to Fab-mediated neutralization provides greater insight into vaccine efficacy for vulnerable populations, such as the elderly, against SARS-CoV-2 and novel variants.

INTRODUCTION

Neutralizing antibody responses are among the core measures of vaccine efficacy in the COVID-19 pandemic (Garcia-Beltran et al., 2022; Liu et al., 2021). Yet, even when neutralization is compromised in the setting of new severe acute respiratory syndrome coronavirus 2 (SARS-CoV-2) variants (Planas et al., 2022; Noori et al., 2022) and cases of vaccine breakthrough infections rise, protection from hospitalization remains relatively high (Altarawneh et al., 2022; Collie et al., 2022; Nasreen et al., 2022; Tang et al., 2021). Thus, the continued emergence of new variants highlights the need to understand vaccine efficacy through protection from disease in addition to prevention of infection.

Though one of the key components of immune protection, the complexity of polyclonal antibody responses and its roles in disease remain only partially understood. For SARS-CoV-2, attention has focused on leveraging direct neutralization of virus by antigen recognition via the Fab domain. However, the overall magnitude of neutralizing responses in patients with severe COVID-19 is higher compared with mild disease, suggesting that neutralizing activity alone poorly captures the capacity to protect from serious illness (Lucas et al., 2021; Savage et al., 2021). Independently, data from multiple large clinical trials have demonstrated that convalescent plasma carrying neutralizing activity does not prevent infection or disease in humans (Begin et al., 2021; RECOVERY Collaborative Group, 2021; Writing Committee for the REMAP-CAP Investigators et al., 2021), suggesting that passive transfer of neutralizing polyclonal antibodies is insufficient to confer protection. These lines of evidence show that in SARS-CoV-2 infection, more nuanced evaluations of neutralizing responses with respect to potency (Garcia-Beltran et al., 2021) and dynamics (Lucas et al., 2021) and immune responses beyond neutralization are vital in understanding pathogenesis.

Antibodies function through the combination of the Fab domain, which directs neutralizing activity against microbial targets, and the Fc domain, which induces non-neutralizing functions (Lu et al., 2018). Through binding Fc receptors expressed on innate and adaptive immune cells as well as activation of

complement, antibody Fc domains have the ability to induce a spectrum of host responses directed against an antigen recognized by the Fab domain (Pincetic et al., 2014). Thus, antibody Fc effector functions have the potential to impact outcomes of SARS-CoV-2 infection and protection in vaccines.

Studies using monoclonal antibodies targeting SARS-CoV-2 show that Fc effector functions can be protective. Passive transfer of monoclonal antibodies with mutations that abrogate Fc domain binding to Fc receptors result in increased SARS-CoV-2 viral load and decreased survival in multiple animal models when compared with intact antibodies (Schafer et al., 2021; Suryadevara et al., 2021; Ullah et al., 2021; Yamin et al., 2021). This effect is more pronounced with therapeutic than with prophylactic administration (Winkler et al., 2021). Thus, monoclonal antibody Fc functions support neutralizing activity to prevent viral entry. Moreover, even after viral infection, Fc functions can inhibit disease progression.

Conversely, several lines of evidence show that Fc effector functions in polyclonal responses during SARS-CoV-2 infection could be pathogenic. Post-translational immunoglobulin G (IgG) glycosylation is altered with disease severity in many ways (Farkash et al., 2021; Petrovic et al., 2021; Vicente et al., 2022), but one consistent observation across several studies is that decreased IgG fucosylation correlates with worsening clinical symptoms and hospitalization (Chakraborty et al., 2021, 2022; Larsen et al., 2021). The proposed mechanism of pathology is through increased binding to the activating Fc receptor FcγRIIIa/CD16a. In an *in vitro* poly I:C-stimulated human macrophage model with FcγRIIIa/CD16a expression, addition of afucosylated, compared with fucosylated, IgG from patients infected with SARS-CoV-2 enhances secretion of the pro-inflammatory cytokine interleukin-6 (IL-6) (Hoepel et al., 2021; Larsen et al., 2021). In monocytes, FcγR-mediated activation can cause pyroptosis (Junqueira et al., 2022). In a human Fc receptor transgenic mouse model, passive transfer of afucosylated polyclonal IgG from individuals with severe COVID-19 increases production of IL-6 and tumor necrosis factor α (TNFα) but not the anti-inflammatory IL-10 (Chakraborty et al., 2022). Consistent with these data, FcγRIIIa/CD16a natural killer (NK) cell activation that leads to antibody-dependent cellular cytotoxicity (ADCC) is enhanced with symptom severity and normalizes upon convalescence (Chakraborty et al., 2021). The low-affinity activating FcγRIIa/CD32a and inhibitory FcγRIIb/CD32b along with the high-affinity FcγRI/CD64 mediate the non-neutralizing Fc effector functions of antibody-dependent cellular phagocytosis (ADCP) by monocytes. Neutrophils express antibody receptors for both IgG, the activating high-affinity FcγRI, and low-affinity FcγRIIa and FcγRIIIB, as well as IgA, the low-affinity FcαRI. These, along with complement receptors CR1 and CR3, contribute to neutrophil phagocytosis. Finally, C1q binding to IgG and IgM Fc domains activates complement pathways through C3 deposition (Lofano et al., 2018; Peschke et al., 2017; Quast et al., 2015; van Osch et al., 2021). In contrast to FcγRIIIa/CD16a activities, the implications of FcγRIIa/CD32a- and FcγRIIb/CD32b-mediated phagocytosis and complement activation in SARS-CoV-2 are less clear given the variability in cohort populations with respect to clinical outcomes, demographics, and co-morbidities (Adeniji et al., 2021; Bartsch et al., 2021; Herman et al., 2021; Klingler et al., 2021; Selva et al., 2021). However, that multiple Fc effector functions in infection and disease are detectable suggest that these responses, if induced by vaccines, could influence outcomes.

For COVID-19 vaccines, neutralizing titers are often used to extrapolate protective efficacy (Lustig et al., 2021). While antibody-dependent NK cell activation (ADNKA), ADCC, ADCP by monocytes, antibody-dependent neutrophil phagocytosis (ADNP) by neutrophils, and complement activation are also elicited (Alter et al., 2021; Gorman et al., 2021; Kaplonek et al., 2022), it is unclear whether these Fc effector functions are protective, inert, or pathogenic. Moreover, how non-neutralizing antibody functions impact direct neutralization of live virus is not known. To assess the relationships between Fab and Fc domain functions in polyclonal responses from vaccination, we evaluated immune sera from SARS-CoV-2-uninfected healthcare workers who received two doses of the BNT162b2 mRNA vaccine. We assessed neutralization against SARS-CoV-2 wild-type virus (WA.1) and five clinical variants: Alpha (B.1.1.7), Beta (B.1.351), Gamma (P.1), Delta (B.1.617.2), and Omicron (BA.2). We measured vaccine-specific antibody Fc features of isotype, Fc receptor binding, Fc effector functions, and IgG glycosylation. We found heterogeneous neutralizing and non-neutralizing antibody responses. Neutralization across variants correlated with FcγRIIIa/CD16a effector functions in an age-, but not sex-, dependent manner. Post-translational afucosylation and sialylation of vaccine-specific antibodies associated with enhanced FcγRIIIa/CD16a activity. Neutralizing and non-neutralizing functions independently and collectively diminished with age, limiting polyfunctional breadth, magnitude, and coordination in those ≥65 years old compared with those <65. Our results show that assessment of vaccine efficacy against SARS-CoV-2 and novel variants is enhanced by the addition of diverse Fc functions to traditional Fab functions, particularly in vulnerable populations such as the elderly.

RESULTS

Study subjects

To evaluate polyclonal antibody responses to mRNA COVID-19 vaccines, sera were collected from 51 adults who received two doses of the BNT162b2 vaccine between December 2020 and February 2021 (Table 1) (Bates et al., 2021a). These individuals spanned a spectrum of ages from 21 to 82 years. To limit confounding variables, samples were selected to minimize variations in time between vaccine doses 1 and 2 (20–22 days, variation of 2 days) and dose 2 to sample collection (14–15 days, variation of 1 day); sex distribution was balanced. To avoid the complicating factor of hybrid immunity due to SARS-CoV-2 infection, we excluded individuals with report of prior infection or active symptoms and performed confirmatory testing to verify the absence of detectable SARS-CoV-2 nucleocapsid specific antibodies (Figure S1A).

Neutralizing antibody titers of wild type and SARS-CoV-2 variants

Using the SARS-CoV-2 receptor-binding domain (RBD) antigen encoded by BNT162b2 (Vogel et al., 2021), we found that

Table 1. Demographics and vaccination status

BNT162b2-vaccinated donors	
Characteristic	total (n = 51)
Median age (range), years	50 (21–82)
Sex	
Female (%)	28 (54.9)
Male (%)	23 (45.1)
Median time between vaccine doses (range), days	21 (20–22)
Median time between second dose and sample collection (range), days	14 (14–15)

100% of individuals after two doses of the vaccine had detectable antigen-specific IgG compared with 51% with IgA (Figure S1A). Thus, consistent with other studies, the primary isotype mediating antibody function 2 weeks after a second BNT162b2 dose was IgG (Brewer et al., 2022; Collier et al., 2021). To assess direct neutralization, we performed focus reduction neutralization tests using live wild-type SARS-CoV-2 (isolate WA1/2020) virus (Figure S1B). Consistent with the generation of RBD-specific IgG, all individuals had detectable capacity to neutralizing activity. Linear regression showed that neutralization was dependent on RBD-specific antibodies, specifically IgG and not IgA (Figure 1A).

We next measured the neutralizing activity of vaccinee sera against SARS-CoV-2 clinical isolates of the viral variants Alpha (B.1.1.7), Beta (B.1.351), Gamma (P.1), Delta (B.1.617.2), and Omicron (BA.2), (Wang et al., 2022) (Figure S1B). We used live virus instead of pseudovirus to more effectively model physiological ratios and spectrum of SARs-CoV-2 antigens during infection and replication (Syed et al., 2021). We found that neutralization of variants was diminished relative to wild type and varied by viral variant and individual (Figure 1B), with the lowest levels detected against Omicron (BA.2), consistent with other studies (Evans et al., 2022; Kurhade et al., 2022; Wang et al., 2022). More specifically, while all individuals had detectable neutralization against wild type and Alpha (B.1.1.7), only 57% had detectable responses against Omicron (BA.2), which were lower on average than for other variants. While sex can impact immune responses (Scully et al., 2020), we observed no sex-based difference in neutralization (Figure S1C). However, we did detect a negative correlation between age and neutralization (Figure S1D). To incorporate both age and sex into our evaluations, we used multivariable regression to assess the relationships with neutralization. We found that neutralization of wild type and variants was negatively correlated with age (Figures 1C–1H), but the correlation with sex remained non-significant. Upon review of the 43% of individuals with no detectable neutralizing activity against Omicron (BA.2), we observed that the median age of this subgroup was 63.5 years, above the median age of 50 for all individuals in this study. Consistent with other reports, these data showed that BNT162b2 induced RBD IgG neutralized SARS-CoV-2 wild-type virus and multiple variants in an age-, but not sex-, dependent manner (Bates et al., 2021a; Collier et al., 2021; Kawasuji et al., 2021).

Vaccine-specific Fc effector functions

Because IgG was the predominant vaccine-specific isotype, we focused on RBD-specific IgG effector functions to evaluate the relationship between viral neutralization via by the Fab domain and non-neutralizing Fc activity. We began by measuring RBD-specific antibody binding to the activating receptors FcγRIIIa/CD16a and FcγRIIa/CD32a and the sole inhibitory receptor FcγRIIb/CD32b because engagement of these low-affinity Fc receptors is modifiable by dynamic changes in subclass and post-translational glycosylation (Alter et al., 2018; Nimmerjahn and Ravetch, 2005; Pincetic et al., 2014). We found that RBD-specific IgG binding to FcγRIIIa/CD16a (Figure 2A), FcγRIIa/CD32a (Figure 2B), and FcγRIIb/CD32b (Figure 2C) positively correlated with SARS-CoV-2 neutralization in varying degrees.

Because Fc domain engagement is only the first step in signaling and initiation of effector functions, we examined the downstream consequences of activation by measuring RBD ADNKA, which leads to ADCC (Chung et al., 2015), ADCP and ADCP, and antibody-dependent complement deposition (ADCD). We found that neutralization titers positively correlated with all three markers of ADNKA: CD107a degranulation and intracellular interferon gamma (IFNγ) and TNF-α production (Figures 2D–2F). This association was not observed with ADNP (Figure 2G) and ADCP (Figure S2A) and was less statistically significant with C3 deposition in ADCD (Figure S2A). Because the primary Fc receptor that induces ADNKA is FcγRIIIa/CD16a, these findings corroborated data with respect to binding (Figure 2A). In contrast, the combinatorial engagement of low- and high-affinity FcγRs and the FcαR on neutrophils in ADNP did not correlate with neutralization (Figure 2G). Along these lines, the ratio of activating FcγRIIa/CD32a and, to a lesser degree, FcγRIIIa/CD16a to the inhibitory FcγRIIb/CD32b involved in ADCP in THP-1 monocytes did not relate to neutralization (Figures S2A and 2H). The link between FcγRIIIa/CD16a NK cell activation and neutralization was sustained across variants, though fits again varied (Figures 2H and S2B). These data together demonstrated that in contrast to FcγRIIa/CD32a and FcγRIIb/CD32b, vaccine-specific IgG induction of FcγRIIIa/CD16a functions associated with neutralization.

IgG glycosylation

As in many infectious and non-infectious processes, post-translational glycosylation of polyclonal IgG has been shown to mediate binding affinity to Fc receptors in SARS-CoV-2 infection (Chakraborty et al., 2021, 2022; Hoepel et al., 2021; Larsen et al., 2021). A core biantennary structure on the conserved asparagine residue N297 on the Fc domain is modified by the addition and subtraction of galactose (G), sialic acid (S), fucose (F), and bisecting N-acetylglucosamine (GlcNAc) to generate glycoform diversity (Arnold et al., 2007) (Figure S3A). Monoclonal and polyclonal antibody studies have shown that changes in glycoform composition have the potential to impact binding and downstream effector functions (Figure S3A) (Alter et al., 2018; Arnold et al., 2007; Peschke et al., 2017; Quast et al., 2015; van Osch et al., 2021). To evaluate the impact of glycosylation on vaccine-induced antibodies, we measured

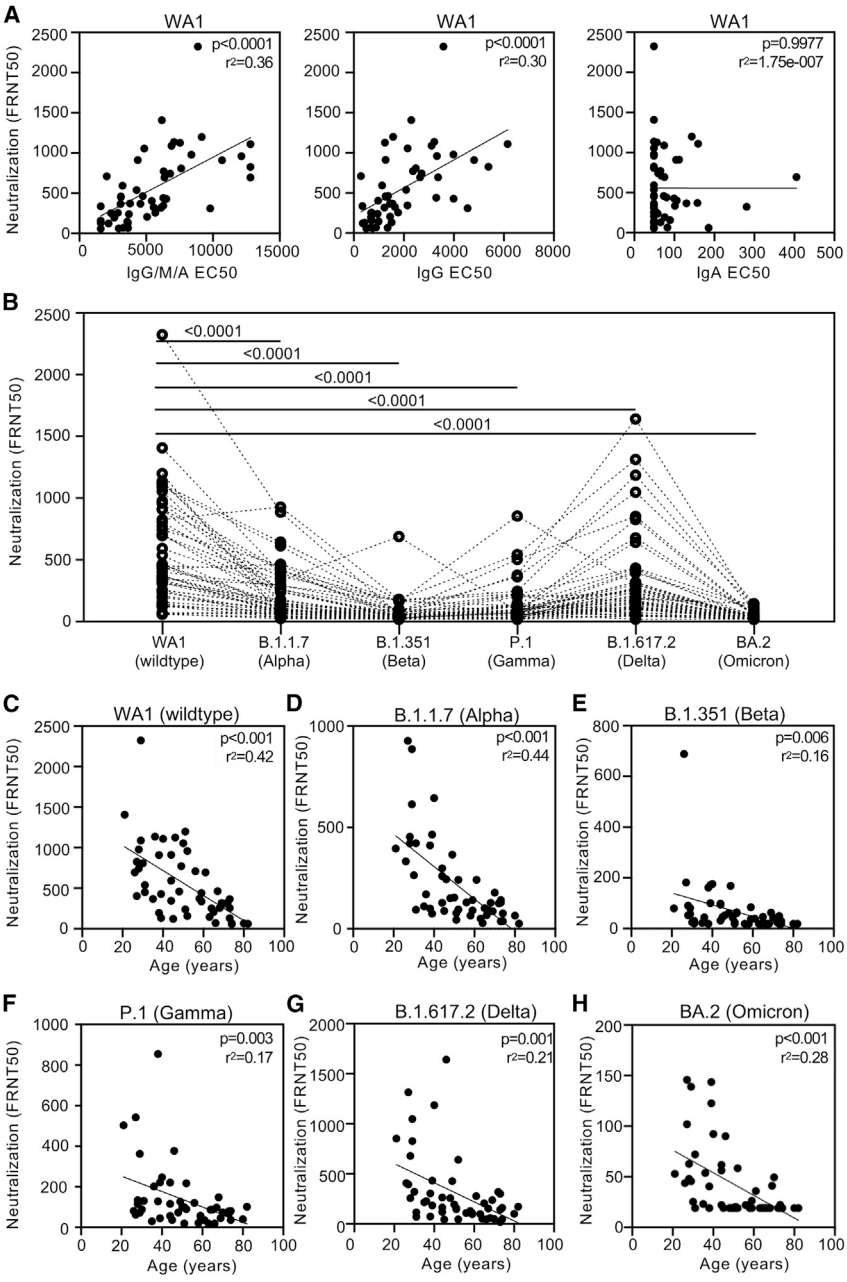

Figure 1. BNT162b2-induced IgG mediates age-dependent neutralization of WT and SARS-CoV-2 clinical variants

(A) Live SARS-CoV-2 neutralization (FRNT50) wild-type WA1 and receptor-binding domain (RBD)-specific IgG/M/A, IgG, and IgA EC50 values (Figure S1A) are plotted with relationship assessed by linear regression.

(B) Neutralization of live SARS-CoV-2 wild-type WA1 and variants (Figure S1B) are depicted, with each dotted line representing a single individual and statistical significance calculated by Wilcoxon matched pair signed rank test.

(C–H) Live SARS-CoV-2 neutralization (FRNT50) for (C) WT and variants (D) B.1.1.7 (Alpha) (n = 50), (E) B.1.351 (Beta) (n = 50), (F) P.1 (Gamma) (n = 50), (G) B.1.617.2 (Delta), and (H) BA.2 (Omicron) and age in years are plotted, with relationship assessed by linear regression and p values adjusted for sex.

Data show the average of technical duplicates for n = 51 individuals' serum samples.

See also Figure S1.

the relative abundance of N-glycans on total non-antigen- and RBD-specific IgG (Figure S3B). For each individual, non-antigen- compared with RBD-specific IgG glycoforms were distinct (Figures 3A and 3B). Glycoforms (Figure S3C) containing fucose (Figure 3C), total sialic (Figure 3D) composed of di-sialic (Figure 3E) and mono-sialic (Figure 3F) acids, galactose (di-galactosylated in Figure 3G and agalactosylated and mono-galactosylated in Figure S3D), and bisecting GlcNAc (Figure S3E) were significantly different between total non-antigen- and RBD-specific IgG.

To evaluate if differential antibody glycosylation impacted effector functions associated with neutralization, we investigated which glycoforms lead to FcγRIIIa/CD16a-mediated NK cell activation by linear regression. We found that relative levels of RBD-, and not total non-antigen-, specific IgG glycoforms significantly correlated with CD107a degranulation and intracellular IFNγ and TNF-α production at varying levels (Figures S4A–S4D). Relative levels of IgG glycoforms that contained fucose without sialic acid (asialylated fucosylated) and glycoforms that contained sialic acid (specifically di-sialic and not mono-sialic acid) correlated with all three markers of NK cell activation (Figures 3H–3K). The negative relationship between asialylated fucosylated species on RBD-specific IgG with ADNKA indicated an inhibitory effect of the presence of fucose. This contrasted with sialic acid, where the absence negatively (Figures 3H and S4E–S4H) and the presence positively (Figures 3I, 3J, S4F, S4G, S4I, and S4J) associated with ADNKA. Taken together, these data showed that fucose and sialic acid on vaccine-specific IgG influence FcγRIIIa/CD16a NK cell activation in opposing manners.

Impact of age on antibody Fc effector functions

We next investigated if Fc domain features were dependent on age as we had observed with Fab domain-mediated neutralization. We observed a negative relationship between RBD-specific IgG binding to FcγRIIIa/CD16a, FcγRIIa/CD32a, and FcγRIIb/CD32b with age (Figures 4A–4C) by linear regression, taking sex into account (Figure 4D). In contrast, no statistically significant relationships between age and Fc receptor binding to antibodies targeting control

Please cite this article in press as: Bates et al., BNT162b2-induced neutralizing and non-neutralizing antibody functions against SARS-CoV-2 diminish with age, Cell Reports (2022), https://doi.org/10.1016/j.celrep.2022.111544

CellPress
OPEN ACCESS

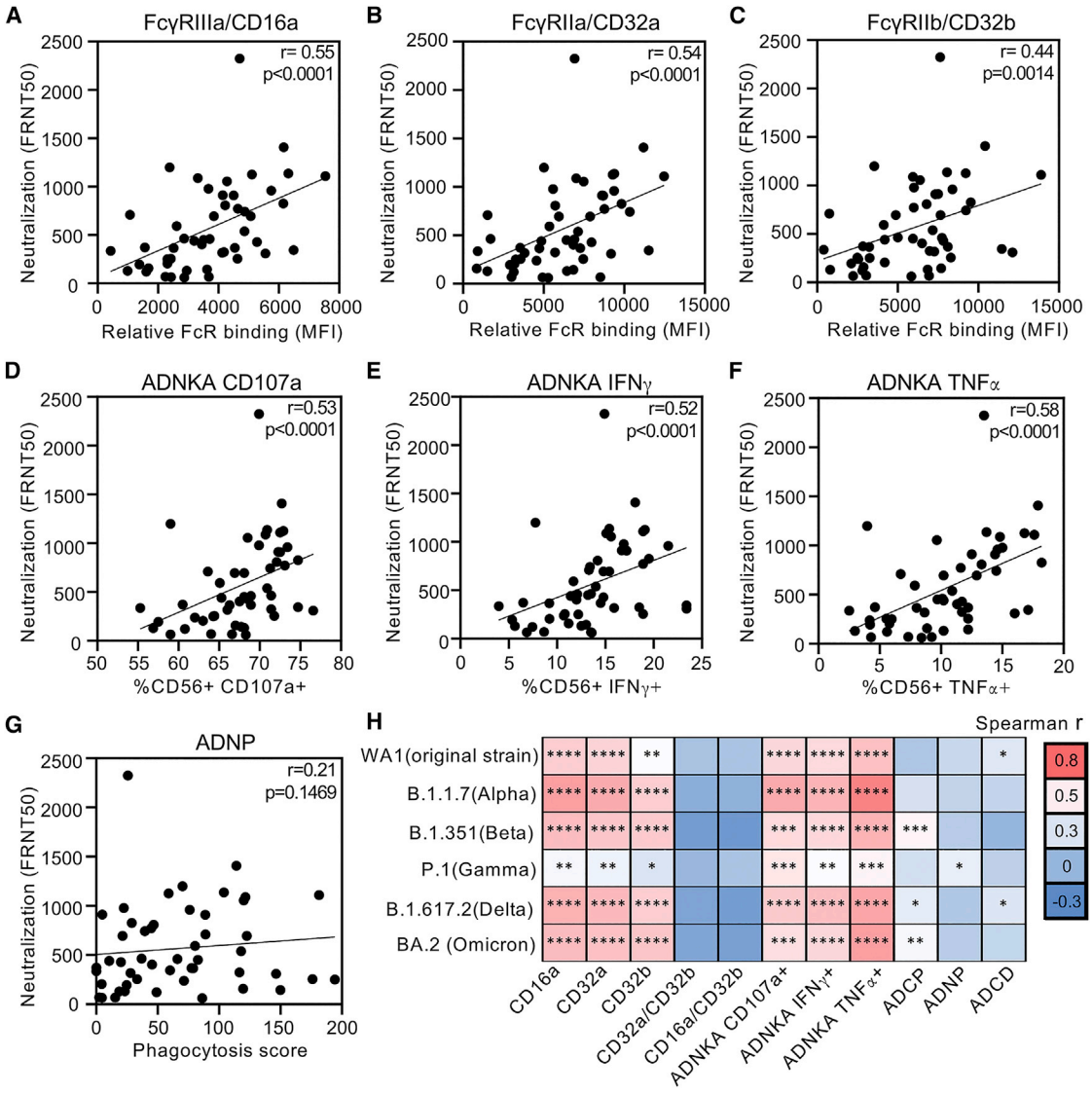

Figure 2. Vaccine-specific IgG induction of FcγRIIIa/CD16a effector functions correlate with neutralization of WT and SARS-CoV-2 clinical variants

(A–G) Relationships between live SARS-CoV-2 WA1 neutralization (FRNT50) and RBD-specific relative binding to (A) FcγRIIIa/CD16a, (B) FcγRIIa/CD32a, and (C) FcγRIIb/CD32b, RBD-specific antibody-dependent natural killer cell activation (ADNKA) determined by (D) CD107a expression, (E) IFNγ production, (F) TNF-α secretion, and (G) RBD-specific antibody-dependent neutrophil phagocytosis (ADNP) are shown.

(H) Heatmap summarizes Spearman correlations (Figure S2) between neutralization of SARS-CoV-2 WT WA1 and variants with relative binding of RBD-specific IgG to activating (FcγRIIIa/CD16a and FcγRIIa/CD32a), inhibitory (FcγRIIb/CD32b), and ratios of activating:inhibitory FcγR (FcγRIIIa/CD16a:FcγRIIb/CD32b and FcγRIIa/CD32a:FcγRIIb/CD32b) binding and Fc effector functions ADNKA, antibody-dependent cellular phagocytosis (ADCP), ADNP, and antibody-dependent complement deposition (ADCD). *p ≤ 0.05; **p ≤ 0.01; ***p ≤ 0.001; ****p ≤ 0.0001.

Depicted here are data representing one of three dilutions with the highest signal to noise ratio for n = 51 individuals' serum samples.

See also Figure S2.

antigens from the other pulmonary viruses respiratory syncytial virus (RSV) and influenza (flu) and the negative control *Bacillus anthracis* (anthrax) were seen (Figure 4D). Consistent with neutralization data, we observed that age negatively correlated with RBD-specific IgG-mediated NK cell CD107a degranulation (Figure 4E) and intracellular IFNγ and TNF-α production at varying levels (Figures S5 and 4F). In comparison, the relationships between age and RBD-specific ADCP (Figure 4G) and ADNP (Figure 4H), as well as ADCD (Figure S5), were non-significant. Consistent with differential IgG glycosylation linked to NK cell activation (Figure 3), asialylated fuosylated glycoforms in RBD-, compared with non-antigen-, specific IgG were increased in those ≥65 years old (Figure 4I). These data showed that age negatively impacted some, but not all, Fc effector functions, as it did for neutralization, which is likely due to the combination of decreased antibody levels

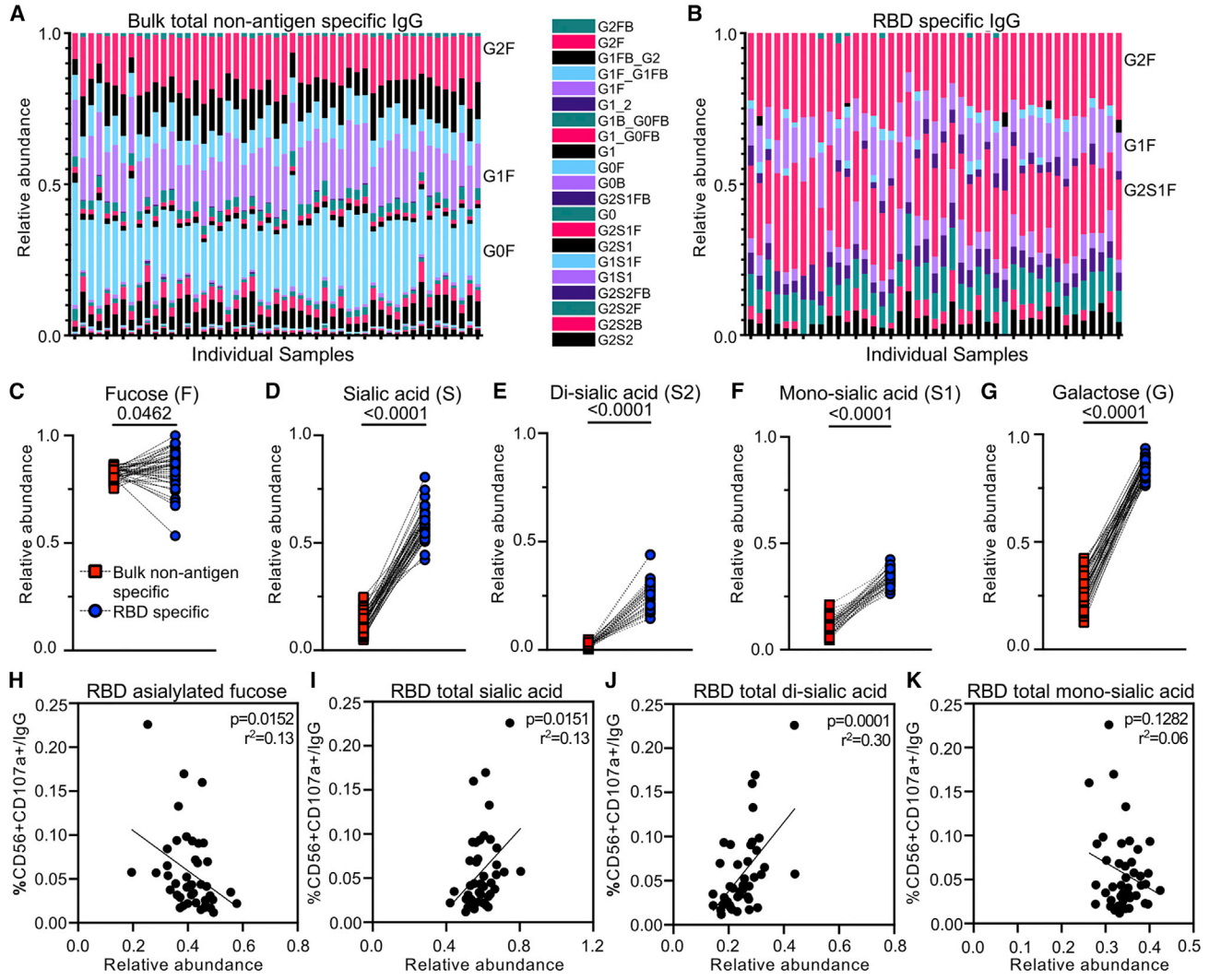

Figure 3. Differential fucose and sialic acid on vaccine-specific IgG link to FcγRIIIa/CD16a effector functions

(A and B) Stacked column graphs depict the relative abundance of individual glycoforms (Figures S3A and S3B) with respect to (A) total bulk non-antigen-specific and (B) RBD-specific IgG. Each column represents one individual study participant.

(C–G) Dot plots summarize differences between bulk non-antigen-specific and RBD-specific IgG in the collective relative abundance of all individual glycoforms (Figures S3C and S3D) containing (C) fucose, (D) total sialic acid, (E) di-sialic acid, (F) mono-sialic acid, and (G) di-galactose, with statistical significance calculated by Wilcoxon matched-pairs signed rank test.

(H–J) Data for (H) asialylated fucosylated, (I) total sialic acid, and (J) total di-sialic acid, the three RBD-specific glycoforms that have a statistically significant relationship across all markers of ADNKA are plotted with CD107a expression per RBD-specific IgG, as well as IFNγ and TNF-α (Figure S4).

(K) For comparison, data for total mono-sialic acid are plotted.

Depicted here are data representing one of three dilutions with the highest signal-to-noise ratio for n = 51 individuals' serum samples.

See also Figures S3 and S4.

and reduced antibody quality in differential glycosylation and altered FcR engagement.

Polyclonal functional breadth and magnitude

Polyclonal antibody responses consist of multiple Fab and Fc domain features that interact to influence disease outcomes. To begin to assess the collective functionality for each vaccinee sample, we calculated the breadth of neutralization across all five SARS-CoV-2 isolates tested (Figure S5A). In addition, we *Z* score-transformed data from Fc assays to enable comparisons between effector functions and summarization of the cumulative Fc functional magnitude for each individual (Figure S5B). To assess how Fc functionality related to Fab activity, we grouped individuals by their neutralization breadth. We found that neutralization of all variants (100%) was detectable in 28 of the 51 individuals, and those remaining demonstrated 50%–83% breadth (Figure 5A). Of those with <100% neutralization breadth, the cumulative Fc functional scores were low or negative. Of those with 100% neutralization breadth, both positive and negative cumulative Fc functional

Please cite this article in press as: Bates et al., BNT162b2-induced neutralizing and non-neutralizing antibody functions against SARS-CoV-2 diminish with age, Cell Reports (2022), https://doi.org/10.1016/j.celrep.2022.111544

CellPress
OPEN ACCESS

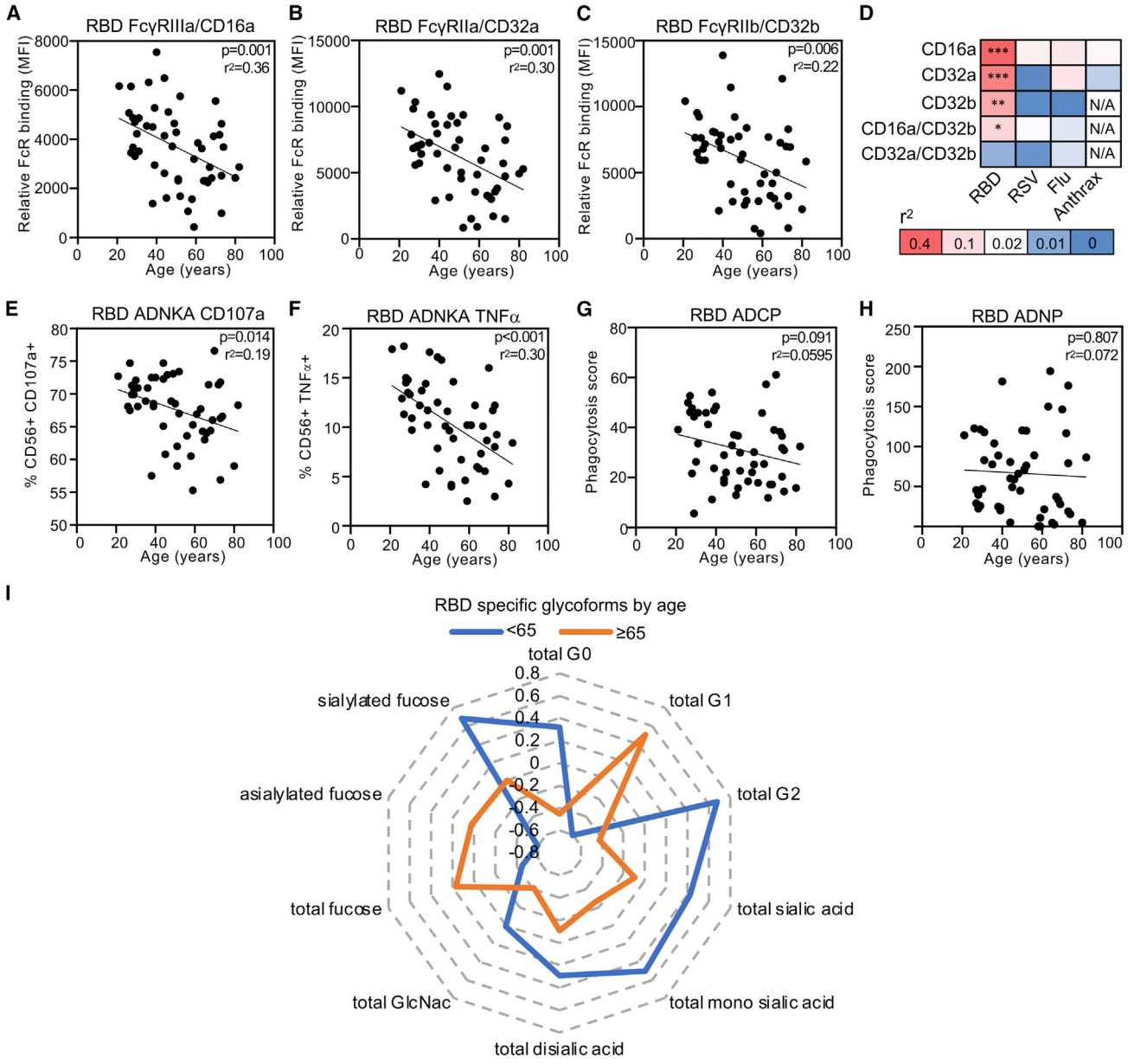

Figure 4. Age influences some, but not all, vaccine-specific antibody FcγR functions

(A–C) The relationships between relative binding of RBD-specific IgG to (A) FcγRIIIa/CD16a, (B) FcγRIIa/CD32a, and (C) inhibitory FcγRIIb/CD32b and age are shown.

(D) Heatmap of the coefficient of determination (r^2) summarizes the goodness of fit across RBD and control respiratory syncytial virus (RSV), influenza (flu), and anthrax antigens in FcγR binding and age. *$p \leq 0.05$; **$p \leq 0.01$; ***$p \leq 0.001$; N/A, not available given absence of significant detectable levels.

(E–H) The relationship between age and RBD ADNKA as measured by (E) CD107a and (F) TNF-α and (G) ADCP and (H) RBD ADNP are shown. Linear regression with p values adjusted for sex are reported.

(I) Radar plots depict vaccine-specific IgG glycoforms calculated from the *Z* scored data for each individual RBD-specific IgG glycoform relative to bulk non-antigen-specific IgG glycoforms, with lines representing the median for each age group.

Depicted here are data representing one of three dilutions with the highest signal-to-noise ratio for n = 51 individuals' serum samples.

See also Figure S5.

scores were detected. Thus, high neutralization breadth and potent Fc effector functions are linked. Moreover, Fc functionality represented a source of immune variation in the presence of broad Fab-mediated neutralization.

Because we observed that both neutralizing (Figure 1) and non-neutralizing (Figure 4) antibody functions were dependent on age, we assessed age with respect to neutralization breadth. We found that the median age for those with 100% neutralization

Please cite this article in press as: Bates et al., BNT162b2-induced neutralizing and non-neutralizing antibody functions against SARS-CoV-2 diminish with age, Cell Reports (2022), https://doi.org/10.1016/j.celrep.2022.111544

was younger (39 years) compared with those with <100% (64.5, 67.5, and 52 years for 50%, 67%, and 83% neutralization, respectively) (Figure 5A). Thus, both antibody Fab- and Fc-mediated breadth and potency diminished with age.

To focus on age categorically, we grouped individuals into those <65 and ≥65. The cutoff of 65 years was chosen for three reasons: (1) 63.5 is the median age of the subgroup of individuals with no detectable neutralization against Omicron (BA.2), the variant with the lowest overall activities (Figure 1B), (2) the median ages of the two groups with the lowest neutralization breadths are 64.5 and 67.5 (Figure 5A), and (3) ≥65 is the definition of older adults used by the Center for Disease Control and Prevention with respect to COVID-19 vaccine administration guidelines (Bialek et al., 2020). We calculated the polyfunctional breadth for each vaccinee by enumerating the proportion of detectable SARS-CoV-2 neutralizing and non-neutralizing responses to categorize individuals as high, medium, and low responders (Figure S5C). We observed that most individuals <65 had high polyfunctional breadth while those ≥65 had low or medium (Figure 5B). This difference in breadth was not noted with groupings by sex (Figure 5C). In addition to antibody breadth, we evaluated polyfunctional magnitude using vaccine-specific neutralizing and non-neutralizing antibody *Z* score data. We found that the extent of all antibody functions, except for ADCP, was diminished in the ≥65, compared with the <65, group (Figure 5D). Because polyfunctional antibody responses are comprised of multiple activities that potentially occur concurrently to influence outcomes of infection, we assessed the coordination between antibody features and functions in these two age groups. We found more coordination in those <65 compared with those ≥65 (Figure 5E). Thus, the breadth, magnitude, and coordination of BNT162b2-induced neutralizing and non-neutralizing antibody polyfunctionality diverge with respect to the age of 65 years.

DISCUSSION

In this study, we show that two doses of the BNT162b2 mRNA vaccine elicited coordinated neutralizing and non-neutralizing antibody functions. The presence of vaccine-specific antibodies is critical, but neutralizing and non-neutralizing antibody functions are driven by quality as well as quantity. Thus, titers correlated with neutralizing activity (Figure 1A) and vaccine-induced neutralizing responses against live clinical isolates of SARS-CoV-2 and five distinct variants decreased with age (Figure 1B). Neutralization correlated with FcγRIIIa/CD16a activation of NK cells that leads to cellular cytotoxicity but not phagocytosis or complement deposition (Figure 2). Engagement with FcγRIIIa/CD16a was associated with post-translational vaccine-specific IgG afucosylation and sialylation (Figures 3H–3K), which diverge with age (Figure 4I). Antibody functions were diminished among those aged ≥65: neutralization breadth across variants, overall Fc functional potency, and coordination between neutralizing and non-neutralizing antibody activities (Figures 5B, 5D, and 5E), demonstrating compromised vaccine-induced polyfunctionality. Neutralizing activity and antibody titers are measured in vaccine studies to gauge effectiveness at blocking infection. The findings from this study show that non-neutralizing antibody effector functions are immune correlates that could inform on the potential of vaccines to prevent disease, a target that is of growing importance with the continual emergence of new variants that subvert neutralization.

Non-neutralizing antibody functions are mediated by immune complexing and binding between the Fc domain and Fc receptors. Thus, even with reduced Fab domain avidity for mutated viral proteins such as spike, vaccine-induced non-neutralizing Fc functions could remain robust. Our data show that neutralizing activities across all variants are lower compared with wild-type virus (Figure 1B), suggesting that effectiveness in preventing infection is significantly compromised. However, even with increased case numbers of infection due to variants, epidemiological data show relatively strong vaccine protection against disease and hospitalization (Altarawneh et al., 2022; Andrews et al., 2022; Collie et al., 2022; Nasreen et al., 2022; Tang et al., 2021). Our data show that the correlation between titers and neutralizing activities was decreased across different variants and that the relationships with non-neutralizing functions, specifically ADNKA, partially overlapped (Figure 5E).

In line with these observations from human studies, data from animal models demonstrate that *in vitro* neutralization does not uniformly correlate with *in vivo* protection against disease (Schafer et al., 2021). Moreover, enhancement of non-neutralizing Fc effector functions delay viral spread synergistically with neutralizing activity in mice (Beaudoin-Bussieres et al., 2022). In humans, our results show that many non-neutralizing Fc effector functions are elicited by vaccination but ADNKA, which leads to cellular cytotoxicity, is specifically linked to neutralization across wild type and SARS-CoV-2 variants (Figure 2). Thus, along with inhibiting viral entry by neutralization, vaccine-specific antibodies via FcγRIIIa/CD16a-expressing NK cells, monocytes, and macrophages could target cytotoxicity against airway epithelial cells already infected with SARS-CoV-2 to prevent viral spread and disease.

In natural infection, FcγRIIIa/CD16a is associated with disease severity (Chakraborty et al., 2021, 2022; Hoepel et al., 2021; Junqueira et al., 2022; Larsen et al., 2021). While our data here do not include individuals with severe COVID-19 disease, the nature of polyclonal antibodies generated during natural infection diverge from vaccination. First, the antigenic repertoire after natural infection likely contains non-RBD-specific antibody responses that are absent after vaccination. Second, antibody titers are likely diminished with exposure to lower amounts of antigen from mild and asymptomatic infection compared with severe disease and vaccination (Dufloo et al., 2021). Thus, FcγRIIIa/CD16a activities from immunity generated after natural infection could confer different downstream consequences compared with vaccination.

Post-translational IgG glycosylation influences Fc receptor binding and activation. Along with afucosylation, which enhances FcγRIIIa/CD16a engagement that is also observed in severe COVID-19 disease, our data from whole vaccine-specific IgG show that sialic acid could also contribute (Figures 3H and 5). As such, sialylation on vaccine-specific IgG could further modify FcγRIIIa/CD16a activation. The study of IgG glycosylation has focused primarily on N297 of the Fc domain (Chakraborty et al., 2021, 2022; Farkash et al., 2021; Hoepel et al.,

Please cite this article in press as: Bates et al., BNT162b2-induced neutralizing and non-neutralizing antibody functions against SARS-CoV-2 diminish with age, Cell Reports (2022), https://doi.org/10.1016/j.celrep.2022.111544

CellPress
OPEN ACCESS

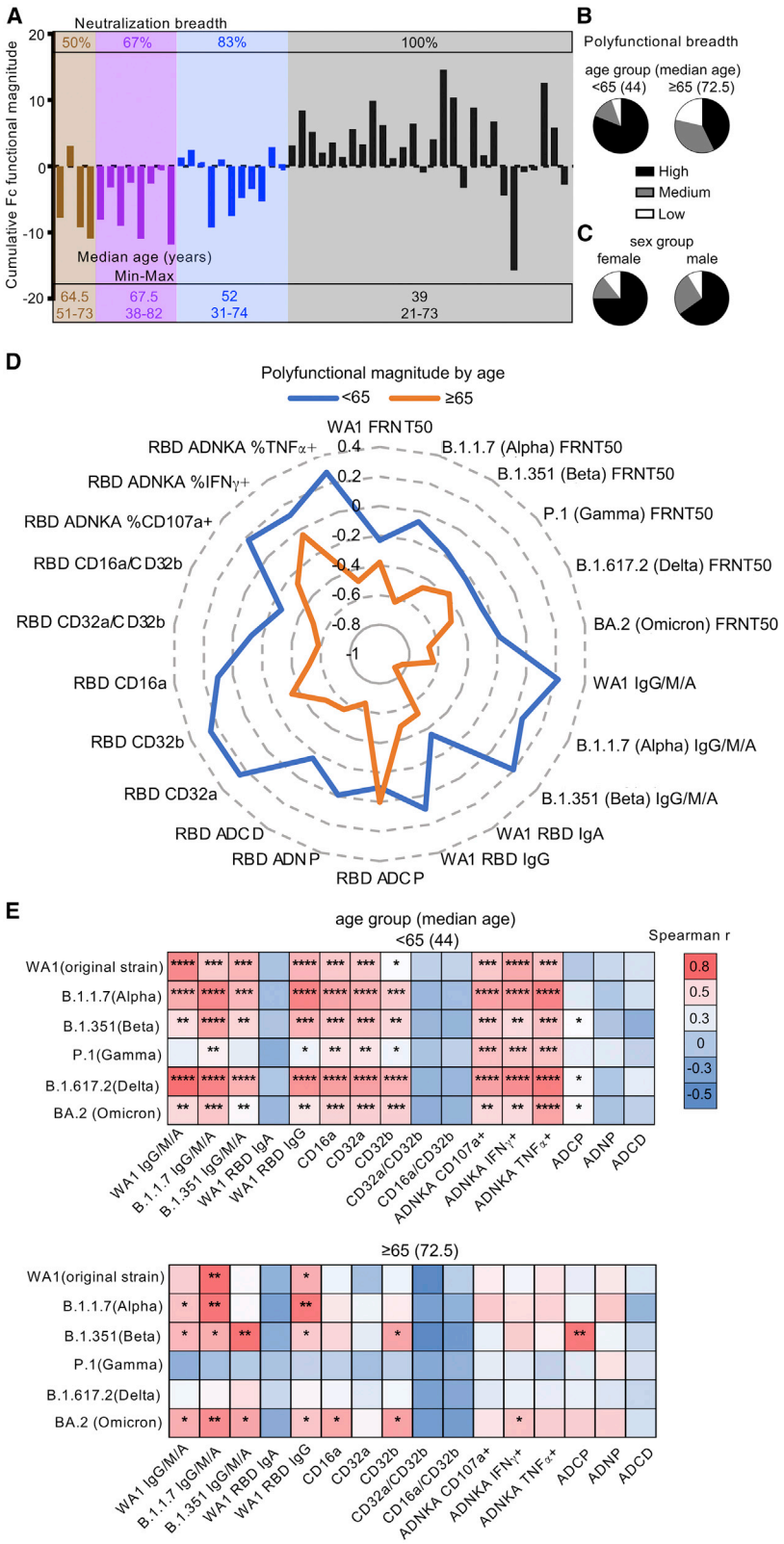

Figure 5. Enhanced BNT162b2 induced polyfunctional antibody breadth and magnitude against SARS-CoV-2 in younger, compared with older, adults

For each individual, the neutralization breadth across variants (Figure S6A) and cumulative vaccine-specific Fc functional magnitude from the sum of the *Z* scores for each of the individual effector functions (Figure S6B) were calculated.

(A) Grouped by neutralization breadth (top), each column shows the cumulative Fc functional score for one individual. Median, minimum, and maximum ages characterizing each neutralization breadth group are shown (bottom). Polyfunctional antibody breadth was calculated for each individual (Figure S6C) and used to categorize individuals into high (90%–100%), medium (80%–90%), or low (<80%) responders.

(B and C) The proportions of high, medium, and low responders are grouped by (B) age and (C) sex.

(D) Radar plots depict vaccine-specific polyfunctional antibody magnitude calculated from the *Z* scored data for each antibody function (Figure S6C), with lines representing the median for each age group.

(E) Heatmap summarizes Spearman correlations (Figure S2) between neutralization of SARS-CoV-2 WT WA1 and variants with RBD-specific IgG/M/A, IgG, and IgA levels, relative binding of RBD-specific IgG to activating (FcγRIIIa/CD16a and FcγRIIa/CD32a), inhibitory (FcγRIIb/CD32b), and ratios of activating:inhibitory FcγR (FcγRIIIa/CD16a:FcγRIIb/CD32b and FcγRIIa/CD32a:FcγRIIb/CD32b) binding, and Fc effector functions ADNKA, ADCP, ADNP, and ADCD for each age group. *p ≤ 0.05; **p ≤ 0.01; ***p ≤ 0.001; ****p ≤ 0.0001.

Depicted here are data representing one of three dilutions with the highest signal-to-noise ratio for n = 51 individuals' serum samples.

See also Figures S2 and S6.

2021; Larsen et al., 2021), not accounting for the 20% of polyclonal IgG modified on the Fab domain (van de Bovenkamp et al., 2016). Our evaluation of whole IgG suggests that glycans from both Fab and Fc domains contribute to Fc effector functions by indirectly and directly affecting Fc receptor interactions (He et al., 2016; Shi et al., 2019; Yamaguchi et al., 2022). Thus, how an Fc receptor is activated by differential antibody glycosylation could be critical in determining the outcomes of downstream immune responses.

The factors that predict vaccine response at an individual level are the subject of intense study. Several lines of evidence support that age is one important factor (Bates et al., 2021a; Collier et al., 2021; Farkash et al., 2021). Our study was designed to look specifically at the contribution of age to non-neutralizing antibody activities from vaccination. In the elderly, compared with younger individuals, virus-specific memory B cells and antibody titers persist longer than neutralizing activity (Jeffery-Smith et al., 2022). Thus, loss of neutralization with a shift toward more dependence on non-neutralizing antibody activity could be a hallmark of immunosenescence. As such, monitoring non-neutralizing, in addition to neutralizing, functions could help determine the need and dose of booster vaccinations for this population. Moreover, approaches using adjuvants to enhance vaccine-mediated non-neutralizing antibody functions such as FcγRIIIa/CD16a could be beneficial (Coler et al., 2018).

With respect to the broader population, analyses of longitudinal and cross-sectional studies involving vaccination and infection show that non-neutralizing functions including NK cell activity and ADCC are sustained longer than neutralization (Fuentes-Villalobos et al., 2022; Lee et al., 2021; Tso et al., 2021). Modeling of neutralization decay predicts that protection from infection is lost but protection from severe disease is retained (Khoury et al., 2021). This divergence between neutralizing titers and immune protection is likely due to multiple factors including viral fitness (Mlcochova et al., 2021; Wang et al., 2021; Weisblum et al., 2020) and T cell activities (Keeton et al., 2022), as well as non-neutralizing responses such as the FcγRIIIa/CD16a functions observed here. Thus, enhancing non-neutralizing activities elicited by vaccines could provide longer-lasting protection against disease independent of altering vaccine antigens to target each new variant.

Current CDC vaccine recommendations for healthy adults <50 involve three total doses and, for those ≥50, four doses. At the time of this writing, 91.8% of the US population ≥65 have received two doses, 70.4% three, and 39.1% four (CDC, 2022). Outside the US, many parts of the world still have limited access to vaccine and have lower rates of vaccination. Our data support the assertion that for those elderly individuals with two doses of BNT162b2, immunity is suboptimal because neutralizing and non-neutralizing antibody activities are restricted. The effects of additional doses of vaccines using antigens from the original SARS-CoV-2 strain or Omicron and infection on top of vaccination that generates hybrid immunity remain to be fully defined but likely encompass enriched neutralization breadth and Fc potency (Collier et al., 2021; Farkash et al., 2021; Richardson et al., 2022). How much protection is enhanced is a subject of active discourse (Atmar et al., 2022; Regev-Yochay et al., 2022). Evaluating the breadth, magnitude, and coordination of polyclonal antibody functions (Figure 5) will enhance resolution of correlates of protection, particularly in the context of variants where the effect of neutralizing activity is likely limited. There is growing evidence that adjuvants and antigens can be used to skew immune responses, including antibody glycosylation and Fc effector functions, for rational vaccine design (Bartsch et al., 2020; Boudreau et al., 2020; Mahan et al., 2016; Oefner et al., 2012). Approaches that leverage the collaboration between antibody Fab and Fc domain functions could improve vaccine efficacy against variants for all and specifically for vulnerable populations with difficulty generating neutralizing responses such as the elderly.

Limitations of the study

Limitations to this study include sample size, a lack of ethnicity, race, and clinical data, and the homogeneity of the population examined, with all participants being employees of a local healthcare system. These cohort characteristics limited the ability to resolve more subtle differences and extrapolate across a diverse array of individuals but also minimized potential sources of confounding variables, likely facilitating the discovery of relationships between antibody features that would otherwise be difficult to discern due to the complexity and heterogeneity of polyfunctional antibodies. The absence of infection was not determined by molecular microbiological diagnostics but rather serologically by the lack of detectable nucleocapsid (Figure S1A), RBD-specific antibodies prior to vaccination (Bates et al., 2021a), and clinical history. As such, it is plausible that individuals with asymptomatic infections are included. However, the dominant immune responses measured were likely due to vaccination given the narrow window between the second vaccine dose and sample collection time (14–15 days). As the cohort was sex balanced, the major known phenotypic variation in this group was age (21–82 years).

STAR★METHODS

Detailed methods are provided in the online version of this paper and include the following:

- KEY RESOURCES TABLE
- RESOURCE AVAILABILITY
  - Lead contact
  - Materials availability
  - Data and code availability
- EXPERIMENTAL MODEL AND SUBJECT DETAILS
  - Cohort
  - Cell lines
  - Primary immune cells
- METHOD DETAILS
  - Virus
  - Enzyme linked immunosorbent assays (ELISA)
  - Focus reduction neutralization test (FRNT)
  - Fc receptor binding assays
  - Non-antigen and RBD-specific IgG glycosylation
  - Antibody dependent cellular phagocytosis (ADCP)
  - Antibody dependent neutrophil phagocytosis (ADNP)
  - Antibody dependent complement deposition (ADCD)

- Antibody dependent NK cell activation (ADNKA)
- QUANTIFICATION AND STATISTICAL ANALYSIS

SUPPLEMENTAL INFORMATION

Supplemental information can be found online at https://doi.org/10.1016/j.celrep.2022.111544.

ACKNOWLEDGMENTS

This study was funded by a grant from the M. J. Murdock Charitable Trust (to M.E.C.); an unrestricted grant from the OHSU Foundation (to M.E.C.); NIH training grant T32HL083808 (to T.A.B.); NIH grant R011R01AI141549-01A1 (to F.G.T.); OHSU Innovative IDEA grant 1018784 (to F.G.T.); NIH grant R01AI145835 (to W.B.M.); Burroughs Wellcome Fund UT Southwestern Training Resident Doctors as Innovators in Science (to Y.J.K.); and a pilot project grant from the UT Southwestern Department of Internal Medicine and Disease Oriented Scholars Award (to L.L.L.). We gratefully acknowledge the OHSU workforce members who participated in this study; the OHSU COVID-19 serology study team and the OHSU occupational health department for their efforts in recruitment and sample acquisition; and the OHSU clinical laboratory under the direction of Donna Hansel and Xuan Qin for SARS-CoV-2 testing and reporting. We thank UTSW healthy volunteers who donated their blood for neutrophil studies; Dawn Wetzel for efforts in recruitment; Gabrielle Lessen for phlebotomy assistance; and Ann McDonald, Gabrielle Lessen, and Joshua Miles for graphical assistance. We are grateful for the support of the M.J. Murdock Charitable Trust and the OHSU Foundation. The funders of the study had no role in study design, execution, analysis, interpretation, or writing of this manuscript.

AUTHOR CONTRIBUTIONS

L.L.L. and F.G.T. conceived, designed, and supervised the work. T.A.B. and P.L. designed, conducted, and analyzed experiments. M.E.C., W.B.M., D.S., and S.K.M. coordinated sample and reagent collection. S.K.M. acquired and analyzed data. Y.J.K., M.T., C.P., and D.K. analyzed the data. L.L.L., F.G.T., T.A.B., and P.L. wrote the manuscript. Y.J.K., M.T., S.K.M., D.K., W.B.M., and M.E.C. contributed to manuscript revisions.

DECLARATION OF INTERESTS

The authors declare no competing interests.

Received: April 16, 2022
Revised: August 12, 2022
Accepted: September 30, 2022
Published: October 25, 2022

REFERENCES

Adeniji, O.S., Giron, L.B., Purwar, M., Zilberstein, N.F., Kulkarni, A.J., Shaikh, M.W., Balk, R.A., Moy, J.N., Forsyth, C.B., Liu, Q., et al. (2021). COVID-19 severity is associated with differential antibody Fc-mediated innate immune functions. mBio *12*, e00281-21. https://doi.org/10.1128/mbio.00281-21.

Altarawneh, H.N., Chemaitelly, H., Ayoub, H.H., Tang, P., Hasan, M.R., Yassine, H.M., Al-Khatib, H.A., Smatti, M.K., Coyle, P., Al-Kanaani, Z., et al. (2022). Effects of previous infection and vaccination on symptomatic Omicron infections. N. Engl. J. Med. *387*, 21–34. https://doi.org/10.1056/nejmoa2203965.

Alter, G., Ottenhoff, T.H.M., and Joosten, S.A. (2018). Antibody glycosylation in inflammation, disease and vaccination. Semin. Immunol. *39*, 102–110. https://doi.org/10.1016/j.smim.2018.05.003.

Alter, G., Yu, J., Liu, J., Chandrashekar, A., Borducchi, E.N., Tostanoski, L.H., McMahan, K., Jacob-Dolan, C., Martinez, D.R., Chang, A., et al. (2021). Immunogenicity of Ad26.COV2.S vaccine against SARS-CoV-2 variants in humans. Nature *596*, 268–272. https://doi.org/10.1038/s41586-021-03681-2.

Andrews, N., Tessier, E., Stowe, J., Gower, C., Kirsebom, F., Simmons, R., Gallagher, E., Thelwall, S., Groves, N., Dabrera, G., et al. (2022). Duration of protection against mild and severe disease by Covid-19 vaccines. N. Engl. J. Med. *386*, 340–350. https://doi.org/10.1056/nejmoa2115481.

Arnold, J.N., Wormald, M.R., Sim, R.B., Rudd, P.M., and Dwek, R.A. (2007). The impact of glycosylation on the biological function and structure of human immunoglobulins. Annu. Rev. Immunol. *25*, 21–50. https://doi.org/10.1146/annurev.immunol.25.022106.141702.

Atmar, R.L., Lyke, K.E., Deming, M.E., Jackson, L.A., Branche, A.R., El Sahly, H.M., Rostad, C.A., Martin, J.M., Johnston, C., Rupp, R.E., et al. (2022). Homologous and heterologous Covid-19 booster vaccinations. N. Engl. J. Med. *386*, 1046–1057. https://doi.org/10.1056/nejmoa2116414.

Bartsch, Y.C., Eschweiler, S., Leliavski, A., Lunding, H.B., Wagt, S., Petry, J., Lilienthal, G.M., Rahmöller, J., de Haan, N., Hölscher, A., et al. (2020). IgG Fc sialylation is regulated during the germinal center reaction following immunization with different adjuvants. J. Allergy Clin. Immunol. *146*, 652–666.e11. https://doi.org/10.1016/j.jaci.2020.04.059.

Bartsch, Y.C., Wang, C., Zohar, T., Fischinger, S., Atyeo, C., Burke, J.S., Kang, J., Edlow, A.G., Fasano, A., Baden, L.R., et al. (2021). Humoral signatures of protective and pathological SARS-CoV-2 infection in children. Nat. Med. *27*, 454–462. https://doi.org/10.1038/s41591-021-01263-3.

Bates, T.A., Leier, H.C., Lyski, Z.L., Goodman, J.R., Curlin, M.E., Messer, W.B., and Tafesse, F.G. (2021a). Age-dependent neutralization of SARS-CoV-2 and P.1 variant by vaccine immune serum samples. JAMA *326*, 868. https://doi.org/10.1001/jama.2021.11656.

Bates, T.A., Leier, H.C., Lyski, Z.L., McBride, S.K., Coulter, F.J., Weinstein, J.B., Goodman, J.R., Lu, Z., Siegel, S.A.R., Sullivan, P., et al. (2021b). Neutralization of SARS-CoV-2 variants by convalescent and BNT162b2 vaccinated serum. Nat. Commun. *12*, 5135. https://doi.org/10.1038/s41467-021-25479-6.

Bates, T.A., Weinstein, J.B., Farley, S., Leier, H.C., Messer, W.B., and Tafesse, F.G. (2021c). Cross-reactivity of SARS-CoV structural protein antibodies against SARS-CoV-2. Cell Rep. *34*, 108737. https://doi.org/10.1016/j.celrep.2021.108737.

Beaudoin-Bussières, G., Chen, Y., Ullah, I., Prévost, J., Tolbert, W.D., Symmes, K., Ding, S., Benlarbi, M., Gong, S.Y., Tauzin, A., et al. (2022). A Fc-enhanced NTD-binding non-neutralizing antibody delays virus spread and synergizes with a nAb to protect mice from lethal SARS-CoV-2 infection. Cell Rep. *38*, 110368. https://doi.org/10.1016/j.celrep.2022.110368.

Bégin, P., Callum, J., Jamula, E., Cook, R., Heddle, N.M., Tinmouth, A., Zeller, M.P., Beaudoin-Bussières, G., Amorim, L., Bazin, R., et al. (2021). Convalescent plasma for hospitalized patients with COVID-19: an open-label, randomized controlled trial. Nat. Med. *27*, 2012–2024. https://doi.org/10.1038/s41591-021-01488-2.

CDC COVID-19 Response Team; Boundy, E., Bowen, V., Chow, N., Cohn, A., Dowling, N., Ellington, S., Gierke, R., Hall, A., MacNeil, J., et al. (2020). Severe outcomes among patients with coronavirus disease 2019 (COVID-19) — United States, February 12–March 16, 2020. MMWR Morb. Mortal. Wkly. Rep. *69*, 343–346. https://doi.org/10.15585/mmwr.mm6912e2.

Boudreau, C.M., Yu, W.H., Suscovich, T.J., Talbot, H.K., Edwards, K.M., and Alter, G. (2020). Selective induction of antibody effector functional responses using MF59-adjuvanted vaccination. J. Clin. Invest. *130*, 662–672. https://doi.org/10.1172/jci129520.

Brewer, R.C., Ramadoss, N.S., Lahey, L.J., Jahanbani, S., Robinson, W.H., and Lanz, T.V. (2022). BNT162b2 vaccine induces divergent B cell responses to SARS-CoV-2 S1 and S2. Nat. Immunol. *23*, 33–39. https://doi.org/10.1038/s41590-021-01088-9.

Brown, E.P., Dowell, K.G., Boesch, A.W., Normandin, E., Mahan, A.E., Chu, T., Barouch, D.H., Bailey-Kellogg, C., Alter, G., and Ackerman, M.E. (2017). Multiplexed Fc array for evaluation of antigen-specific antibody effector profiles. J. Immunol. Methods *443*, 33–44. https://doi.org/10.1016/j.jim.2017.01.010.

CDC (2022). COVID-19 vaccinations in the United States. In COVID Data Tracker (US Department of Health and Human Services, CDC: Center for Disease Control and Prevention).

Chakraborty, S., Gonzalez, J., Edwards, K., Mallajosyula, V., Buzzanco, A.S., Sherwood, R., Buffone, C., Kathale, N., Providenza, S., Xie, M.M., et al. (2021). Proinflammatory IgG Fc structures in patients with severe COVID-19. Nat. Immunol. *22*, 67–73. https://doi.org/10.1038/s41590-020-00828-7.

Chakraborty, S., Gonzalez, J.C., Sievers, B.L., Mallajosyula, V., Chakraborty, S., Dubey, M., Ashraf, U., Cheng, B.Y.L., Kathale, N., Tran, K.Q.T., et al. (2022). Early non-neutralizing, afucosylated antibody responses are associated with COVID-19 severity. Sci. Transl. Med. *14*, eabm7853. https://doi.org/10.1126/scitranslmed.abm7853.

Chung, A.W., Kumar, M.P., Arnold, K.B., Yu, W.H., Schoen, M.K., Dunphy, L.J., Suscovich, T.J., Frahm, N., Linde, C., Mahan, A.E., et al. (2015). Dissecting polyclonal vaccine-induced humoral immunity against HIV using Systems serology. Cell *163*, 988–998. https://doi.org/10.1016/j.cell.2015.10.027.

Coler, R.N., Day, T.A., Ellis, R., Piazza, F.M., Beckmann, A.M., Vergara, J., Rolf, T., Lu, L., Alter, G., Hokey, D., et al. (2018). The TLR-4 agonist adjuvant, GLA-SE, improves magnitude and quality of immune responses elicited by the ID93 tuberculosis vaccine: first-in-human trial. NPJ Vaccines *3*, 34. https://doi.org/10.1038/s41541-018-0057-5.

Collie, S., Champion, J., Moultrie, H., Bekker, L.G., and Gray, G. (2022). Effectiveness of BNT162b2 vaccine against Omicron variant in South Africa. N. Engl. J. Med. *386*, 494–496. https://doi.org/10.1056/nejmc2119270.

Collier, D.A., Ferreira, I.A.T.M., Kotagiri, P., Datir, R.P., Lim, E.Y., Touizer, E., Meng, B., Abdullahi, A., CITIID-NIHR BioResource COVID-19 Collaboration; and Elmer, A., et al. (2021). Age-related immune response heterogeneity to SARS-CoV-2 vaccine BNT162b2. Nature *596*, 417–422. https://doi.org/10.1038/s41586-021-03739-1.

Darrah, P.A., Patel, D.T., De Luca, P.M., Lindsay, R.W.B., Davey, D.F., Flynn, B.J., Hoff, S.T., Andersen, P., Reed, S.G., Morris, S.L., et al. (2007). Multifunctional TH1 cells define a correlate of vaccine-mediated protection against Leishmania major. Nat. Med. *13*, 843–850. https://doi.org/10.1038/nm1592.

Dufloo, J., Grzelak, L., Staropoli, I., Madec, Y., Tondeur, L., Anna, F., Pelleau, S., Wiedemann, A., Planchais, C., Buchrieser, J., et al. (2021). Asymptomatic and symptomatic SARS-CoV-2 infections elicit polyfunctional antibodies. Cell Rep. Med. *2*, 100275. https://doi.org/10.1016/j.xcrm.2021.100275.

Evans, J.P., Zeng, C., Qu, P., Faraone, J., Zheng, Y.M., Carlin, C., Bednash, J.S., Zhou, T., Lozanski, G., Mallampalli, R., et al. (2022). Neutralization of SARS-CoV-2 Omicron sub-lineages BA.1, BA.1.1, and BA.2. Cell Host Microbe *30*, 1093–1102. https://doi.org/10.1016/j.chom.2022.04.014.

Farkash, I., Feferman, T., Cohen-Saban, N., Avraham, Y., Morgenstern, D., Mayuni, G., Barth, N., Lustig, Y., Miller, L., Shouval, D.S., et al. (2021). Anti-SARS-CoV-2 antibodies elicited by COVID-19 mRNA vaccine exhibit a unique glycosylation pattern. Cell Rep. *37*, 110114. https://doi.org/10.1016/j.celrep.2021.110114.

Fischinger, S., Fallon, J.K., Michell, A.R., Broge, T., Suscovich, T.J., Streeck, H., and Alter, G. (2019). A high-throughput, bead-based, antigen-specific assay to assess the ability of antibodies to induce complement activation. J. Immunol. Methods *473*, 112630. https://doi.org/10.1016/j.jim.2019.07.002.

Fuentes-Villalobos, F., Garrido, J.L., Medina, M.A., Zambrano, N., Ross, N., Bravo, F., Gaete-Argel, A., Oyarzún-Arrau, A., Amanat, F., Soto-Rifo, R., et al. (2022). Sustained antibody-dependent NK cell functions in mild COVID-19 outpatients during convalescence. Front. Immunol. *13*, 796481. https://doi.org/10.3389/fimmu.2022.796481.

Garcia-Beltran, W.F., Lam, E.C., Astudillo, M.G., Yang, D., Miller, T.E., Feldman, J., Hauser, B.M., Caradonna, T.M., Clayton, K.L., Nitido, A.D., et al. (2021). COVID-19-neutralizing antibodies predict disease severity and survival. Cell *184*, 476–488.e11. https://doi.org/10.1016/j.cell.2020.12.015.

Garcia-Beltran, W.F., St Denis, K.J., Hoelzemer, A., Lam, E.C., Nitido, A.D., Sheehan, M.L., Berrios, C., Ofoman, O., Chang, C.C., Hauser, B.M., et al. (2022). mRNA-based COVID-19 vaccine boosters induce neutralizing immunity against SARS-CoV-2 Omicron variant. Cell *185*, 457–466.e4. https://doi.org/10.1016/j.cell.2021.12.033.

Gorman, M.J., Patel, N., Guebre-Xabier, M., Zhu, A.L., Atyeo, C., Pullen, K.M., Loos, C., Goez-Gazi, Y., Carrion, R., Jr., Tian, J.H., et al. (2021). Fab and Fc contribute to maximal protection against SARS-CoV-2 following NVX-CoV2373 subunit vaccine with Matrix-M vaccination. Cell Rep. Med. *2*, 100405. https://doi.org/10.1016/j.xcrm.2021.100405.

Gunn, B.M., Roy, V., Karim, M.M., Hartnett, J.N., Suscovich, T.J., Goba, A., Momoh, M., Sandi, J.D., Kanneh, L., Andersen, K.G., et al. (2020). Survivors of Ebola virus disease develop polyfunctional antibody responses. J. Infect. Dis. *221*, 156–161. https://doi.org/10.1093/infdis/jiz364.

He, W., Tan, G.S., Mullarkey, C.E., Lee, A.J., Lam, M.M.W., Krammer, F., Henry, C., Wilson, P.C., Ashkar, A.A., Palese, P., and Miller, M.S. (2016). Epitope specificity plays a critical role in regulating antibody-dependent cell-mediated cytotoxicity against influenza A virus. Proc. Natl. Acad. Sci. USA *113*, 11931–11936. https://doi.org/10.1073/pnas.1609316113.

Herman, J.D., Wang, C., Loos, C., Yoon, H., Rivera, J., Eugenia Dieterle, M., Haslwanter, D., Jangra, R.K., Bortz, R.H., 3rd, Bar, K.J., et al. (2021). Functional convalescent plasma antibodies and pre-infusion titers shape the early severe COVID-19 immune response. Nat. Commun. *12*, 6853. https://doi.org/10.1038/s41467-021-27201-y.

Hoepel, W., Chen, H.J., Geyer, C.E., Allahverdiyeva, S., Manz, X.D., de Taeye, S.W., Aman, J., Mes, L., Steenhuis, M., Griffith, G.R., et al. (2021). High titers and low fucosylation of early human anti-SARS-CoV-2 IgG promote inflammation by alveolar macrophages. Sci. Transl. Med. *13*, eabf8654. https://doi.org/10.1126/scitranslmed.abf8654.

Jeffery-Smith, A., Burton, A.R., Lens, S., Rees-Spear, C., Davies, J., Patel, M., Gopal, R., Muir, L., Aiano, F., Doores, K.J., et al. (2022). SARS-CoV-2-specific memory B cells can persist in the elderly who have lost detectable neutralizing antibodies. J. Clin. Invest. *132*, e152042. https://doi.org/10.1172/jci152042.

Junqueira, C., Crespo, Â., Ranjbar, S., de Lacerda, L.B., Lewandrowski, M., Ingber, J., Parry, B., Ravid, S., Clark, S., Schrimpf, M.R., et al. (2022). FcgammaR-mediated SARS-CoV-2 infection of monocytes activates inflammation. Nature *606*, 576–584. https://doi.org/10.1038/s41586-022-04702-4.

Kaplonek, P., Cizmeci, D., Fischinger, S., Collier, A.R., Suscovich, T., Linde, C., Broge, T., Mann, C., Amanat, F., Dayal, D., et al. (2022). mRNA-1273 and BNT162b2 COVID-19 vaccines elicit antibodies with differences in Fc-mediated effector functions. Sci. Transl. Med. *14*, eabm2311. https://doi.org/10.1126/scitranslmed.abm2311.

Katzelnick, L.C., Coello Escoto, A., McElvany, B.D., Chávez, C., Salje, H., Luo, W., Rodriguez-Barraquer, I., Jarman, R., Durbin, A.P., Diehl, S.A., et al. (2018). Viridot: an automated virus plaque (immunofocus) counter for the measurement of serological neutralizing responses with application to dengue virus. PLoS Negl. Trop. Dis. *12*, e0006862. https://doi.org/10.1371/journal.pntd.0006862.

Kawasuji, H., Morinaga, Y., Tani, H., Saga, Y., Kaneda, M., Murai, Y., Ueno, A., Miyajima, Y., Fukui, Y., Nagaoka, K., et al. (2021). Age-dependent reduction in neutralization against Alpha and Beta variants of BNT162b2 SARS-CoV-2 vaccine-induced immunity. Microbiol. Spectr. *9*, e0056121. https://doi.org/10.1128/spectrum.00561-21.

Keeton, R., Tincho, M.B., Ngomti, A., Baguma, R., Benede, N., Suzuki, A., Khan, K., Cele, S., Bernstein, M., Karim, F., et al. (2022). T cell responses to SARS-CoV-2 spike cross-recognize Omicron. Nature *603*, 488–492. https://doi.org/10.1038/s41586-022-04460-3.

Khoury, D.S., Cromer, D., Reynaldi, A., Schlub, T.E., Wheatley, A.K., Juno, J.A., Subbarao, K., Kent, S.J., Triccas, J.A., and Davenport, M.P. (2021). Neutralizing antibody levels are highly predictive of immune protection from symptomatic SARS-CoV-2 infection. Nat. Med. *27*, 1205–1211. https://doi.org/10.1038/s41591-021-01377-8.

Klingler, J., Lambert, G.S., Itri, V., Liu, S., Bandres, J.C., Enyindah-Asonye, G., Liu, X., Simon, V., Gleason, C.R., Kleiner, G., et al. (2021). Detection of antibody responses against SARS-CoV-2 in plasma and saliva from vaccinated and infected individuals. Front. Immunol. *12*, 759688. https://doi.org/10.3389/fimmu.2021.759688.

Kurhade, C., Zou, J., Xia, H., Cai, H., Yang, Q., Cutler, M., Cooper, D., Muik, A., Jansen, K.U., Xie, X., et al. (2022). Neutralization of Omicron BA.1, BA.2, and BA.3 SARS-CoV-2 by 3 doses of BNT162b2 vaccine. Nat. Commun. *13*, 3602. https://doi.org/10.1038/s41467-022-30681-1.

Larsen, M.D., de Graaf, E.L., Sonneveld, M.E., Plomp, H.R., Nouta, J., Hoepel, W., Chen, H.J., Linty, F., Visser, R., Brinkhaus, M., et al. (2021). Afucosylated IgG characterizes enveloped viral responses and correlates with COVID-19 severity. Science *371*, eabc8378. https://doi.org/10.1126/science.abc8378.

Lee, W.S., Selva, K.J., Davis, S.K., Wines, B.D., Reynaldi, A., Esterbauer, R., Kelly, H.G., Haycroft, E.R., Tan, H.X., Juno, J.A., et al. (2021). Decay of Fc-dependent antibody functions after mild to moderate COVID-19. Cell Rep. Med. *2*, 100296. https://doi.org/10.1016/j.xcrm.2021.100296.

Liu, J., Liu, Y., Xia, H., Zou, J., Weaver, S.C., Swanson, K.A., Cai, H., Cutler, M., Cooper, D., Muik, A., et al. (2021). BNT162b2-elicited neutralization of B.1.617 and other SARS-CoV-2 variants. Nature *596*, 273–275. https://doi.org/10.1038/s41586-021-03693-y.

Lofano, G., Gorman, M.J., Yousif, A.S., Yu, W.H., Fox, J.M., Dugast, A.S., Ackerman, M.E., Suscovich, T.J., Weiner, J., Barouch, D., et al. (2018). Antigen-specific antibody Fc glycosylation enhances humoral immunity via the recruitment of complement. Sci. Immunol. *3*, eaat7796. https://doi.org/10.1126/sciimmunol.aat7796.

Lu, L.L., Chung, A.W., Rosebrock, T.R., Ghebremichael, M., Yu, W.H., Grace, P.S., Schoen, M.K., Tafesse, F., Martin, C., Leung, V., et al. (2016). A functional role for antibodies in tuberculosis. Cell *167*, 433–443.e14. https://doi.org/10.1016/j.cell.2016.08.072.

Lu, L.L., Suscovich, T.J., Fortune, S.M., and Alter, G. (2018). Beyond binding: antibody effector functions in infectious diseases. Nat. Rev. Immunol. *18*, 46–61. https://doi.org/10.1038/nri.2017.106.

Lucas, C., Klein, J., Sundaram, M.E., Liu, F., Wong, P., Silva, J., Mao, T., Oh, J.E., Mohanty, S., Huang, J., et al. (2021). Delayed production of neutralizing antibodies correlates with fatal COVID-19. Nat. Med. *27*, 1178–1186. https://doi.org/10.1038/s41591-021-01355-0.

Lustig, Y., Sapir, E., Regev-Yochay, G., Cohen, C., Fluss, R., Olmer, L., Indenbaum, V., Mandelboim, M., Doolman, R., Amit, S., et al. (2021). BNT162b2 COVID-19 vaccine and correlates of humoral immune responses and dynamics: a prospective, single-centre, longitudinal cohort study in health-care workers. Lancet Respir. Med. *9*, 999–1009. https://doi.org/10.1016/s2213-2600(21)00220-4.

Mahan, A.E., Jennewein, M.F., Suscovich, T., Dionne, K., Tedesco, J., Chung, A.W., Streeck, H., Pau, M., Schuitemaker, H., Francis, D., et al. (2016). Antigen-specific antibody glycosylation is regulated via vaccination. PLoS Pathog. *12*, e1005456. https://doi.org/10.1371/journal.ppat.1005456.

Mahan, A.E., Tedesco, J., Dionne, K., Baruah, K., Cheng, H.D., De Jager, P.L., Barouch, D.H., Suscovich, T., Ackerman, M., Crispin, M., and Alter, G. (2015). A method for high-throughput, sensitive analysis of IgG Fc and Fab glycosylation by capillary electrophoresis. J. Immunol. Methods *417*, 34–44. https://doi.org/10.1016/j.jim.2014.12.004.

Mlcochova, P., Kemp, S.A., Dhar, M.S., Papa, G., Meng, B., Ferreira, I.A.T.M., Datir, R., Collier, D.A., Albecka, A., Singh, S., et al. (2021). SARS-CoV-2 B.1.617.2 Delta variant replication and immune evasion. Nature *599*, 114–119. https://doi.org/10.1038/s41586-021-03944-y.

Nasreen, S., Chung, H., He, S., Brown, K.A., Gubbay, J.B., Buchan, S.A., Fell, D.B., Austin, P.C., Schwartz, K.L., Sundaram, M.E., et al. (2022). Effectiveness of COVID-19 vaccines against symptomatic SARS-CoV-2 infection and severe outcomes with variants of concern in Ontario. Nat. Microbiol. *7*, 379–385. https://doi.org/10.1038/s41564-021-01053-0.

Nimmerjahn, F., and Ravetch, J.V. (2005). Divergent immunoglobulin g subclass activity through selective Fc receptor binding. Science *310*, 1510–1512. https://doi.org/10.1126/science.1118948.

Noori, M., Nejadghaderi, S.A., Arshi, S., Carson-Chahhoud, K., Ansarin, K., Kolahi, A.A., and Safiri, S. (2022). Potency of BNT162b2 and mRNA-1273 vaccine-induced neutralizing antibodies against severe acute respiratory syndrome-CoV-2 variants of concern: a systematic review of in vitro studies. Rev. Med. Virol. *32*, e2277. https://doi.org/10.1002/rmv.2277.

Oefner, C.M., Winkler, A., Hess, C., Lorenz, A.K., Holecska, V., Huxdorf, M., Schommartz, T., Petzold, D., Bitterling, J., Schoen, A.L., et al. (2012). Tolerance induction with T cell-dependent protein antigens induces regulatory sialylated IgGs. J. Allergy Clin. Immunol. *129*, 1647–1655.e13. https://doi.org/10.1016/j.jaci.2012.02.037.

Peschke, B., Keller, C.W., Weber, P., Quast, I., and Lünemann, J.D. (2017). Fc-galactosylation of human immunoglobulin gamma isotypes improves C1q binding and enhances complement-dependent cytotoxicity. Front. Immunol. *8*, 646. https://doi.org/10.3389/fimmu.2017.00646.

Petrović, T., Alves, I., Bugada, D., Pascual, J., Vučković, F., Skelin, A., Gaifem, J., Villar-Garcia, J., Vicente, M.M., Fernandes, Â., et al. (2021). Composition of the immunoglobulin G glycome associates with the severity of COVID-19. Glycobiology *31*, 372–377. https://doi.org/10.1093/glycob/cwaa102.

Pincetic, A., Bournazos, S., DiLillo, D.J., Maamary, J., Wang, T.T., Dahan, R., Fiebiger, B.M., and Ravetch, J.V. (2014). Type I and type II Fc receptors regulate innate and adaptive immunity. Nat. Immunol. *15*, 707–716. https://doi.org/10.1038/ni.2939.

Planas, D., Saunders, N., Maes, P., Guivel-Benhassine, F., Planchais, C., Buchrieser, J., Bolland, W.H., Porrot, F., Staropoli, I., Lemoine, F., et al. (2022). Considerable escape of SARS-CoV-2 Omicron to antibody neutralization. Nature *602*, 671–675. https://doi.org/10.1038/s41586-021-04389-z.

Quast, I., Keller, C.W., Maurer, M.A., Giddens, J.P., Tackenberg, B., Wang, L.X., Münz, C., Nimmerjahn, F., Dalakas, M.C., and Lünemann, J.D. (2015). Sialylation of IgG Fc domain impairs complement-dependent cytotoxicity. J. Clin. Invest. *125*, 4160–4170. https://doi.org/10.1172/jci82695.

RECOVERY Collaborative Group (2021). Convalescent plasma in patients admitted to hospital with COVID-19 (RECOVERY): a randomised controlled, open-label, platform trial. Lancet *397*, 2049–2059. https://doi.org/10.1016/s0140-6736(21)00897-7.

Regev-Yochay, G., Gonen, T., Gilboa, M., Mandelboim, M., Indenbaum, V., Amit, S., Meltzer, L., Asraf, K., Cohen, C., Fluss, R., et al. (2022). Efficacy of a fourth dose of Covid-19 mRNA vaccine against Omicron. N. Engl. J. Med. *386*, 1377–1380. https://doi.org/10.1056/nejmc2202542.

Richardson, S.I., Manamela, N.P., Motsoeneng, B.M., Kaldine, H., Ayres, F., Makhado, Z., Mennen, M., Skelem, S., Williams, N., Sullivan, N.J., et al. (2022). SARS-CoV-2 Beta and Delta variants trigger Fc effector function with increased cross-reactivity. Cell Rep. Med. *3*, 100510. https://doi.org/10.1016/j.xcrm.2022.100510.

Savage, H.R., Santos, V.S., Edwards, T., Giorgi, E., Krishna, S., Planche, T.D., Staines, H.M., Fitchett, J.R.A., Kirwan, D.E., Cubas Atienzar, A.I., et al. (2021). Prevalence of neutralising antibodies against SARS-CoV-2 in acute infection and convalescence: a systematic review and meta-analysis. PLoS Negl. Trop. Dis. *15*, e0009551. https://doi.org/10.1371/journal.pntd.0009551.

Schäfer, A., Muecksch, F., Lorenzi, J.C.C., Leist, S.R., Cipolla, M., Bournazos, S., Schmidt, F., Maison, R.M., Gazumyan, A., Martinez, D.R., et al. (2021). Antibody potency, effector function, and combinations in protection and therapy for SARS-CoV-2 infection in vivo. J. Exp. Med. *218*, e20201993. https://doi.org/10.1084/jem.20201993.

Scully, E.P., Haverfield, J., Ursin, R.L., Tannenbaum, C., and Klein, S.L. (2020). Considering how biological sex impacts immune responses and COVID-19 outcomes. Nat. Rev. Immunol. *20*, 442–447. https://doi.org/10.1038/s41577-020-0348-8.

Selva, K.J., van de Sandt, C.E., Lemke, M.M., Lee, C.Y., Shoffner, S.K., Chua, B.Y., Davis, S.K., Nguyen, T.H.O., Rowntree, L.C., Hensen, L., et al. (2021). Systems serology detects functionally distinct coronavirus antibody features in children and elderly. Nat. Commun. *12*, 2037. https://doi.org/10.1038/s41467-021-22236-7.

Shi, L., Liu, T., Gross, M.L., and Huang, Y. (2019). Recognition of human IgG1 by Fcgamma receptors: structural insights from hydrogen-deuterium Exchange and fast photochemical oxidation of proteins coupled with mass spectrometry. Biochemistry *58*, 1074–1080. https://doi.org/10.1021/acs.biochem.8b01048.

Suryadevara, N., Shrihari, S., Gilchuk, P., VanBlargan, L.A., Binshtein, E., Zost, S.J., Nargi, R.S., Sutton, R.E., Winkler, E.S., Chen, E.C., et al. (2021). Neutralizing and protective human monoclonal antibodies recognizing the N-terminal domain of the SARS-CoV-2 spike protein. Cell *184*, 2316–2331.e15. https://doi.org/10.1016/j.cell.2021.03.029.

Syed, A.M., Taha, T.Y., Tabata, T., Chen, I.P., Ciling, A., Khalid, M.M., Sreekumar, B., Chen, P.Y., Hayashi, J.M., Soczek, K.M., et al. (2021). Rapid assessment of SARS-CoV-2-evolved variants using virus-like particles. Science *374*, 1626–1632. https://doi.org/10.1126/science.abl6184.

Tang, P., Hasan, M.R., Chemaitelly, H., Yassine, H.M., Benslimane, F.M., Al Khatib, H.A., AlMukdad, S., Coyle, P., Ayoub, H.H., Al Kanaani, Z., et al. (2021). BNT162b2 and mRNA-1273 COVID-19 vaccine effectiveness against the SARS-CoV-2 Delta variant in Qatar. Nat. Med. *27*, 2136–2143. https://doi.org/10.1038/s41591-021-01583-4.

Tso, F.Y., Lidenge, S.J., Poppe, L.K., Peña, P.B., Privatt, S.R., Bennett, S.J., Ngowi, J.R., Mwaiselage, J., Belshan, M., Siedlik, J.A., et al. (2021). Presence of antibody-dependent cellular cytotoxicity (ADCC) against SARS-CoV-2 in COVID-19 plasma. PLoS One *16*, e0247640. https://doi.org/10.1371/journal.pone.0247640.

Ullah, I., Prévost, J., Ladinsky, M.S., Stone, H., Lu, M., Anand, S.P., Beaudoin-Bussières, G., Symmes, K., Benlarbi, M., Ding, S., et al. (2021). Live imaging of SARS-CoV-2 infection in mice reveals that neutralizing antibodies require Fc function for optimal efficacy. Immunity *54*, 2143–2158.e15. https://doi.org/10.1016/j.immuni.2021.08.015.

van de Bovenkamp, F.S., Hafkenscheid, L., Rispens, T., and Rombouts, Y. (2016). The emerging importance of IgG Fab glycosylation in immunity. J. Immunol. *196*, 1435–1441. https://doi.org/10.4049/jimmunol.1502136.

van Osch, T.L.J., Nouta, J., Derksen, N.I.L., van Mierlo, G., van der Schoot, C.E., Wuhrer, M., Rispens, T., and Vidarsson, G. (2021). Fc galactosylation promotes hexamerization of human IgG1, leading to enhanced classical complement activation. J. Immunol. *207*, 1545–1554. https://doi.org/10.4049/jimmunol.2100399.

Váradi, C., Lew, C., and Guttman, A. (2014). Rapid magnetic bead based sample preparation for automated and high throughput N-glycan analysis of therapeutic antibodies. Anal. Chem. *86*, 5682–5687. https://doi.org/10.1021/ac501573g.

Vicente, M.M., Alves, I., Gaifem, J., Rodrigues, C.S., Fernandes, Â., Dias, A.M., Štambuk, J., Petrović, T., Oliveira, P., Ferreira-da-Silva, F., et al. (2022). Altered IgG glycosylation at COVID-19 diagnosis predicts disease severity. Eur. J. Immunol. *52*, 946–957. https://doi.org/10.1002/eji.202149491.

Vogel, A.B., Kanevsky, I., Che, Y., Swanson, K.A., Muik, A., Vormehr, M., Kranz, L.M., Walzer, K.C., Hein, S., Güler, A., et al. (2021). BNT162b vaccines protect rhesus macaques from SARS-CoV-2. Nature *592*, 283–289. https://doi.org/10.1038/s41586-021-03275-y.

Wang, P., Nair, M.S., Liu, L., Iketani, S., Luo, Y., Guo, Y., Wang, M., Yu, J., Zhang, B., Kwong, P.D., et al. (2021). Antibody resistance of SARS-CoV-2 variants B.1.351 and B.1.1.7. Nature *593*, 130–135. https://doi.org/10.1038/s41586-021-03398-2.

Wang, Q., Guo, Y., Iketani, S., Nair, M.S., Li, Z., Mohri, H., Wang, M., Yu, J., Bowen, A.D., Chang, J.Y., et al. (2022). Antibody evasion by SARS-CoV-2 Omicron subvariants BA.2.12.1, BA.4 and BA.5. Nature *608*, 603–608. https://doi.org/10.1038/s41586-022-05053-w.

Weisblum, Y., Schmidt, F., Zhang, F., DaSilva, J., Poston, D., Lorenzi, J.C., Muecksch, F., Rutkowska, M., Hoffmann, H.H., Michailidis, E., et al. (2020). Escape from neutralizing antibodies by SARS-CoV-2 spike protein variants. Elife *9*, e61312. https://doi.org/10.7554/elife.61312.

Winkler, E.S., Gilchuk, P., Yu, J., Bailey, A.L., Chen, R.E., Chong, Z., Zost, S.J., Jang, H., Huang, Y., Allen, J.D., et al. (2021). Human neutralizing antibodies against SARS-CoV-2 require intact Fc effector functions for optimal therapeutic protection. Cell *184*, 1804–1820.e16. https://doi.org/10.1016/j.cell.2021.02.026.

Writing Committee for the REMAP-CAP Investigators; Abdelhady, H., Abdelrazik, M., Abdi, Z., Abdo, D., Abdulle, A., Abel, L., Abouzeenni, S., Abrahamson, G., Abusamra, Y., et al. (2021). Effect of convalescent plasma on organ support-free days in critically Ill patients with COVID-19: a randomized clinical trial. JAMA *326*, 1690–1702. https://doi.org/10.1001/jama.2021.18178.

Yamaguchi, Y., Wakaizumi, N., Irisa, M., Maruno, T., Shimada, M., Shintani, K., Nishiumi, H., Yogo, R., Yanaka, S., Higo, D., et al. (2022). The Fab portion of immunoglobulin G has sites in the CL domain that interact with Fc gamma receptor IIIa. mAbs *14*, 2038531. https://doi.org/10.1080/19420862.2022.2038531.

Yamin, R., Jones, A.T., Hoffmann, H.H., Schäfer, A., Kao, K.S., Francis, R.L., Sheahan, T.P., Baric, R.S., Rice, C.M., Ravetch, J.V., and Bournazos, S. (2021). Fc-engineered antibody therapeutics with improved anti-SARS-CoV-2 efficacy. Nature *599*, 465–470. https://doi.org/10.1038/s41586-021-04017-w.

Please cite this article in press as: Bates et al., BNT162b2-induced neutralizing and non-neutralizing antibody functions against SARS-CoV-2 diminish with age, Cell Reports (2022), https://doi.org/10.1016/j.celrep.2022.111544

CellPress
OPEN ACCESS

STAR★METHODS

KEY RESOURCES TABLE

REAGENT or RESOURCE	SOURCE	IDENTIFIER
Antibodies		
anti-human GOXHU IgG/A/M-HRP	Invitrogen	Cat#A18847; RRID:AB_2535624
anti-human IgA-HRP	Biolegend	Cat#411002; RRID:AB_2686938
anti-human IgG-HRP	BD Biosciences	Cat#555788; RRID:AB_396123
anti-SARS-CoV-2 alpaca serum	Capralogics	Bates et al. (2021b)
anti-alpaca-HRP	Novus	Cat#NB7242; RRID:AB_524704
Pacific Blue anti-human CD66b Antibody	Biolegend	Cat#305112; RRID:AB_2563294
Alexa Fluor 488 Mouse Anti-Human CD107a (clone H4A3)	BD Biosciences	Cat#328610; RRID:AB_1227504
PE/Cy7 anti-human CD56 (NCAM) (clone 5.1H11)	Biolegend	Cat#362510; RRID:AB_2563927
Pacific Blue Anti-CD16 Mouse anti-Human (clone 3G8)	Biolegend	Cat#302032; RRID:AB_2104003
PE Anti-IFN-γ Mouse anti-Human (clone B27)	Biolegend	Cat#506507; RRID:AB_315440
APC Anti-TNF Mouse anti-Human (clone Mab11)	Biolegend	Cat#502912; RRID:AB_315264
Anti-guinea pig complement C3, goat polyclonal antibody	MP Biomedicals	Cat#0855371; RRID:AB_2334449
Bacterial and virus strains		
SARS-CoV-2 USA-WA1/2020 [original strain]	BEI Resources	NR-52281
SARS-CoV-2 USA/CA_CDC_5574/2020 [B.1.1.7]	BEI Resources	NR-54011
SARS-CoV-2 hCoV-54 19/South Africa/ KRISP-K005325/2020 [B.1.351]	BEI Resources	NR-54009
SARS-CoV-2 hCoV-19/Japan/TY7-503/ 2021 [P.1]	BEI Resources	NR-54982
SARS-CoV-2 hCoV-19/USA/PHC658/2021 [B.1.617.2]	BEI Resources	NR-55611
hCoV-19/USA/CO-CDPHE-2102544747/ 2021 [B.1.1.529 - BA.2]	BEI Resources	NR-56520
Biological samples		
SARS-CoV-2 vaccinated human sera	This study	N/A
Chemicals, peptides, and recombinant proteins		
Recombinant human IL-2	Gibco	Cat#PHC0021
recombinant SARS-CoV-2 spike receptor binding domain	BEI Resources	NR-52309
recombinant SARS-CoV-2 nucleocapsid	BEI Resources	NR-53797
o-phenylenediamine	Thermo Scientific	Cat#34006
Pierce™ EDC, No-Weigh™ Format	Thermo Scientific	Cat#A35391
Sulfo-NHS	Thermo Scientific	Cat#A39269
H1N1 Influenza vaccine	BEI Resources	NR-20083
H1N1 Influenza vaccine	BEI Resources	NR-51702
H5N1 Influenza vaccine	BEI Resources	NR-12148
B Victoria Influenza vaccine	BEI Resources	NR-51702
Anthrax Protective Antigen	BEI Resources	NR-36208

(*Continued on next page*)

Please cite this article in press as: Bates et al., BNT162b2-induced neutralizing and non-neutralizing antibody functions against SARS-CoV-2 diminish with age, Cell Reports (2022), https://doi.org/10.1016/j.celrep.2022.111544

Continued

REAGENT or RESOURCE	SOURCE	IDENTIFIER
Anthrax Lethal Factor	BEI Resources	NR-28544
Anthrax Edema Factor	BEI Resources	NR-36210
Respiratory Syncytial Virus G protein from strain B1	BEI Resources	NR-31098
Respiratory Syncytial Virus F protein from strain B1	BEI Resources	NR-31097
Respiratory Syncytial Virus G protein from strain A2	BEI Resources	NR-31096
Recombinant FcγRIIIa/CD16a	R&D Systems	Cat#4325-FC
Recombinant FcγRIIa/CD32a	R&D Systems	Cat#9595-CD
Recombinant FcγRIIb/CD32b	R&D Systems	Cat#1875-CD
PE/R-Phycoerythrin Conjugation Kit	Abcam	Cat# ab102918
EZ-Link™ Sulfo-NHS-LC-Biotin	Thermo Scientific	Cat#21335
Streptavidin Magnetic Beads	New England Biolabs	Cat#S1420S
PureProteome™ Protein G Magnetic Bead System	Millipore	Cat#LSKMAGG10
PNGase F	New England Biolabs	Cat#P0704S
8-aminoinopyrene-1,3,6-trisulfonic acid	ThermoFisher	Cat#A6257
Guinea pig complement	Cedarlane	Cat#CL4051
brefeldin A	Biolegend	Cat#420601
Golgi Stop	BD Biosciences	Cat#554724
Intracellular Staining Permeabilization Wash Buffer	Biolegend	Cat#421002
Acetonitrile	Fisher Scientific	Cat#A9961
Experimental models: Cell lines		
Vero E6	ATCC	CRL-1586; RRID:CVCL_0574
THP-1	ATCC	TIB-202; RRID:CVCL_0006
CD16.NK-92	ATCC	PTA-6967; RRID:CVCL_V429
Software and algorithms		
Viridot (version 1.0)	Katzelnick et al. (2018)	https://github.com/leahkatzelnick/Viridot
$FRNT_{50}$ calculator (version 1.0)	Bates et al. (2021b)	https://github.com/tbates0/FRNT50_calculator/tree/v1.0
R (version 4.2.1)	R Project	https://www.r-project.org/
Python (version 3.8.13)	Python Software Foundation	https://www.python.org/
GlycanAssure Data Acquisition Software (version 1.0)	Applied Biosystems	Cat#A30467
FlowJo (version 10.8.1)	BD Biosciences	https://www.flowjo.com
Prism (version 9.0)	GraphPad	https://www.graphpad.com/scientific-software/prism/
Stata (version 17)	StataCorp	https://www.stata.com
Other		
MagPlex Microspheres	Luminex corporation	Cat# MC10043-01; MC10034-01; MC10037-01; MC10065-01
Agencourt CleanSEQ beads	Beckman Coulter	Cat#A29154
Bio-Gel P-2 size exclusion resin	Bio-Rad	Cat#1504118
FluoSpheres™ NeutrAvidin™-Labeled Microspheres, 1.0 μm, red fluorescent (580/605), 1% solids	Invitrogen	Cat#F8775
Empty 96-Well Macro SpinColumn with 7 μm frit, 1.1 mL Reservoir Plate	Harvard Apparatus	Cat#74-5649

RESOURCE AVAILABILITY

Lead contact

Further information and requests for resources and reagents should be directed to and will be fulfilled by the lead contact, Lenette Lu (lenette.lu@utsouthwestern.edu).

Materials availability

No unique reagents were generated during the course of this study.

Data and code availability

The dataset generated during this study is available upon reasonable request. This paper does not report original code. Any additional information required to reanalyze the data reported in this paper is available from the lead contact upon request.

EXPERIMENTAL MODEL AND SUBJECT DETAILS

Cohort

Study participants (n = 51) were enrolled between December 2020 and February 2021 at Oregon Health & Science University immediately after receiving their first dose of BNT162b2 vaccine. Cohort age and sex distributions are described in Table 1. Participants received a second vaccine dose between 21 ± 1 day following the first dose, then returned 14-15 days later for follow up. Whole blood was collected in serum tubes (BD) and serum isolated by centrifugation 1000xg for 10min. Sera were heat inactivated at 65°C for 30min then frozen at −20°C. This study was conducted in accordance with the Oregon Health & Science University Institutional Review Board with written informed consent from all participants, and approved by the UT Southwestern Medical Center Institutional Review Board. Written informed consent was received from all study participants prior to participation.

Cell lines

Vero E6 cells were purchased from ATCC (ATCC VERO C1008), grown at 37C, 5% CO2 and maintained in Dulbecco's Modified Eagle Medium supplemented with 10% fetal bovine serum, 1% penicillin/streptomycin, 1% non-essential amino acids. THP-1 cells were purchased from ATCC (ATCC TIB-202), grown at 37C, 5% CO2 and maintained in RPMI-1640 supplemented with 10% fetal bovine serum, 2mM L-glutamine, 10mM HEPES, and 0.05 mM β-mercaptoethanol. CD16.NK-92 were purchased from ATCC (ATCC PTA-6967), grown at 37C, 5% CO2 and maintained in in MEM-α supplemented with 12.5% FBS, 12.5% horse serum, 1.5g/L sodium bicarbonate, 0.02mM folic acid, 0.2mM inositol, 0.1 mM 2-β-mercaptoethanol, 100U/mL recombinant IL-2.

Primary immune cells

Fresh peripheral blood was collected at UT Southwestern from healthy volunteers. All were over 18 and de-identified prior to blood processing. Neutrophils isolated from peripheral blood were maintained at 37C, 5% CO2 in RPMI with 10% fetal bovine serum, L-glutamine, and HEPES. The study was approved by the UT Southwestern Medical Center Institutional Review Board. Written informed consent was received from all study participants prior to participation.

METHOD DETAILS

Virus

SARS-CoV-2 clinical isolates were passaged once before use in neutralization assays: USA-WA1/2020 [original strain] (BEI Resources NR-52281); USA/CA_CDC_5574/2020 [B.1.1.7] (BEI Resources NR-54011); hCoV-54 19/South Africa/KRISP-K005325/2020 [B.1.351] (BEI Resources NR-54009); hCoV-19/Japan/TY7-503/2021 [P.1] (BEI Resources NR-54982); hCoV-19/USA/PHC658/2021 [B.1.617.2] (BEI Resources NR-55611); and hCoV-19/USA/CO-CDPHE-2102544747/2021 [B.1.1.529 - BA.2] (BEI Resources NR-56520). Isolates were propagated in Vero E6 cells for 24 to 72hrs until cultures displayed at least 20% cytopathic effect (CPE), as previously described.

Enzyme linked immunosorbent assays (ELISA)

ELISAs were performed as described (Bates et al., 2021b). Plates were coated overnight at 4°C with 1 mg/mL recombinant SARS-CoV-2 spike receptor binding domain (RBD) protein (Bates et al., 2021c) (BEI Resources NR-52309) or recombinant SARS-CoV-2 nucleocapsid (N) protein (BEI Resources NR-53797). Serum dilutions (6 x 3-fold for RBD, 6 x 4-fold for N) in duplicate were prepared in 5% milk powder, 0.05% Tween 20, in phosphate buffered saline (PBS), starting at 1:1600 (pan-Ig), 1:50 (IgA), 1:200 (IgG). The secondary antibodies used were pan-Ig (1:10,000 anti-human GOXHU IgG/A/M-HRP, A18847 Invitrogen), IgA (1:3,000 anti-human IgA-HRP, 411,002 Biolegend), and IgG (1:3,000 anti-human IgG-HRP 555788, BD Biosciences). Plates were developed with o-phenylenediamine (OPD) (ThermoScientific). Absorbance at 492nm was measured on a CLARIOstar plate reader and normalized by subtracting the average of negative control wells and dividing by the highest concentration from a positive control dilution series. ELISA

EC50 values were calculated by fitting normalized A492 as described (Bates et al., 2021b). The limit of detection (LOD) was defined by the lowest dilution tested for RBD and half of the lowest dilution for N. Values below the LOD were set to LOD – 1.

Focus reduction neutralization test (FRNT)

Focus forming assays were performed as described (Bates et al., 2021b). Sub-confluent Vero E6 cells were incubated for 1 h with 30 μL of diluted sera (5 x 4-fold starting at 1:20) which was pre-incubated for 1 h with 100 infectious viral particles per well. Samples were tested in duplicate. Wells were covered with 150 μL of overlay media containing 1% methylcellulose and incubated for 24hrs, 48hrs for Omicron. Plates were fixed by soaking in 4% formaldehyde in PBS for 1 h at room temperature. After permeabilization with 0.1% BSA, 0.1% saponin in PBS, plates were incubated overnight at 4°C with primary antibody (1:5,000 anti-SARS-CoV-2 alpaca serum, 1:2,000 for Omicron) (Capralogics Inc) (Bates et al., 2021b). Plates were then washed and incubated for 2hrs at room temperature with secondary antibody (1:20,000 anti-alpaca-HRP, 1:5,000 for Omicron) (NB7242 Novus) and developed with TrueBlue (SeraCare) for 30min. Foci were imaged with a CTL Immunospot Analyzer, enumerated using the viridot package (Katzelnick et al., 2018) and percent neutralization calculated relative to the average of virus-only wells for each plate. FRNT50 values were determined by fitting percent neutralization to a 3-parameter logistic model as described previously (Bates et al., 2021b). The limit of detection (LOD) was defined by the lowest dilution tested, values below the LOD were set to LOD – 1. Duplicate FRNT50 values were first calculated separately to confirm values were within 4-fold. When true, a final FRNT50 was calculated by fitting to combined replicates.

Fc receptor binding assays

Fc receptor binding assays were performed as described with modifications (Brown et al., 2017). Carboxylated microspheres (Luminex) were coupled with recombinant SARS-CoV-2 RBD (Bates et al., 2021c) (BEI Resources NR-52309) by covalent NHS-ester linkages via EDC (1-Ethyl-3-[3-dimethylaminopropyl]carbodiimide hydrochloride, Thermo Scientific Pierce) and Sulfo-NHS (N-hydroxysulfosuccinimide) (Thermo Scientific) per the manufacturer's instructions. A mixture of influenza antigens from strain H1N1 (NR-20083 and NR-51702, BEI Resources), H5N1 (NR-12148, BEI Resources), H3N2, B Yamagata lineage, and B Victoria lineage (NR-51702, BEI Resources) was used as a control. A mixture of recombinant *Bacillus anthracis* antigens (Anthrax Protective Antigen, NR-36208 BEI Resources; Anthrax Lethal Factor, NR-28544 BEI Resources; Anthrax Edema Factor, NR-36210 BEI Resources) and a separate mixture of recombinant Respiratory Syncytial Virus antigens (G protein from strain B1, NR-31098 BEI Resources; F protein from strain B1, NR-31097 BEI Resources; G protein from strain A2, NR-31096 BEI Resources) were also used as controls. Antigen-coupled microspheres (1250 beads per well) were incubated with serially diluted sera (1:100, 1:1000, 1:10,000) in 96-well Bioplex Pro Flat Bottom plates (Bio-Rad) at 4°C for 16hrs. Recombinant Fc receptors (FcγRIIIa/CD16a, FcγRIIa/CD32a, FcγRIIb/CD32b, R&D Systems) were fluorescently labeled with PE (Abcam) before addition to bead bound antigen specific immune complexes. After 2hrs of incubation at room temperature, the beads were washed with PBS with 0.05% Tween 20 and antigen specific antibody bound Fc receptor measured on a on a MAGPIX instrument containing xPONENT4.2 software (Luminex). The background signal, defined as MFI of microspheres incubated with PBS, was subtracted. Representative data from one dilution was chosen by the highest signal to noise ratio for further analyses.

Non-antigen and RBD-specific IgG glycosylation

Non-antigen and RBD specific IgG glycans were purified and relative levels quantified as described with modifications (Mahan et al., 2015; Varadi et al., 2014). Recombinant RBD protein (BEI Resources NR-52309) (Bates et al., 2021c) was biotinylated with sulfosuccinimidyl-6-[biotinamido]-6-hexanamido hexanoate (sulfo-NHS-LC-LC biotin; ThermoScientific) and coupled to streptavidin beads (New England Biolabs). Patient sera were incubated with RBD-coupled beads and excess sera washed with PBS (Sigma). Bead-bound RBD-specific antibodies then eluted using 100mM citric acid (pH 3.0) and neutralized with 0.5M potassium phosphate (pH 9.0). Non-antigen specific or RBD-specific IgG were purified from the serum or eluted RBD-specific antibodies respectively by protein G beads (Millipore). Purified IgG was denatured and treated with PNGase enzyme (New England Biolabs) for 12hrs at 37°C to release glycans.

To isolate bulk IgG glycans, proteins were removed by precipitation using ice-cold 100% ethanol at −20°C for 10min. To isolated RBD-specific IgG glycans, Agencourt CleanSEQ beads (Beckman Coulter) were used to bind glycans in 87.5% acetonitrile (Fisher Scientific). The supernatant was removed, glycans eluted from beads with HPLC grade water (Fisher Scientific) and dried by centrifugal force and vacuum (CentriVap). Glycans were fluorescently labeled with a 1.5:1 ratio of 50mM APTS (8-aminoinopyrene-1,3,6-trisulfonic acid, ThermoFisher) in 1.2M citric acid and 1M sodium cyanoborohydride in tetrahydrofuran (Fisher Scientific) at 55°C for 3hrs. The labeled glycans were dissolved in HPLC grade water (Fisher Scientific) and excess unbound APTS was removed using Agencourt CleanSEQ beads and Bio-Gel P-2 (Bio-rad) size exclusion resin. Glycan samples were run with a LIZ 600 DNA ladder in Hi-Di formamide (ThermoFisher) on an ABI 3500xL DNA sequencer and analyzed with GlycanAssure Data Acquisition Software v.1.0. Each glycoform was separated by peaks and identified based on glycan standard libraries (GKSP-520, Agilent). The relative abundance of each glycan for each individual sample was determined as (area under curve of each glycan)/(sum of area under curve of all individual glycans).

Antibody dependent cellular phagocytosis (ADCP)

The THP-1 (TIB-202, ATCC) phagocytosis assay of antigen-coated beads was conducted as described with modifications (Lu et al., 2016). SARS-CoV-2 RBD recombinant protein (BEI Resources NR-52309) (Bates et al., 2021c) was biotinylated with Sulfo-NHS-LC

Biotin (Thermo Fisher), then incubated with 1 μm fluorescent neutravidin beads (Invitrogen) at 4°C for 16hrs. Excess antigen was washed away and RBD-coupled neutravidin beads were resuspended in PBS-0.1% bovine serum albumin (BSA). RBD-coupled beads were incubated with serial dilutions of sera (1:100, 1:500 and 1:2500) for 2hrs at 37°C. THP1 cells (1×10^5 per well) were then added. Plasma opsonized RBD-coupled beads and THP1 cells were incubated at 37°C for 16hrs. Cells were then washed once and fixed with 4% PFA. Bead uptake was measured on a BD LSRFortessa (SCC) equipped with high-throughput sampler and analyzed by FlowJo10. Phagocytic scores were calculated as the integrated median fluorescence intensity (MFI) (% bead-positive frequency × MFI/10,000) (Darrah et al., 2007). Representative data from one dilution was chosen by the highest signal to noise ratio for further analyses.

Antibody dependent neutrophil phagocytosis (ADNP)

The neutrophil phagocytosis assay of antigen-coated beads was conducted as described with modifications (Lu et al., 2016). Whole healthy donor blood was mixed with equal volume 3% dextran-500 (Thermo Fisher) and incubated for 25 min at room temperature to lyse and pellet the red blood cells. Leukocytes were removed and washed in endotoxin-free sterile water (Cytiva), followed by 1.8% NaCl (Thermo scientific) and then Hanks' balanced salt solution without calcium and magnesium (Thermo Fisher). RBD conjugated beads, as described above, were incubated with serial dilution of sera (1:100, 1:500 and 1:2500) in duplicate for 2hrs at 37°C. Isolated neutrophils (1×10^5 per well) were added and incubated for 2hrs at 37°C. Bead uptake was measured on a BD LSRFortessa (SCC) equipped with high-throughput sampler and analyzed by FlowJo10. Phagocytic scores were calculated as the integrated median fluorescence intensity (MFI) (% bead-positive frequency × MFI/1,000). The purity of neutrophils was confirmed by staining with CD66b (BioLegend). Sera samples were tested in two independent experiments with neutrophils from two different HIV negative healthy donors. The mean of the data from both donors was used for further analysis. Representative data from one dilution was chosen by the highest signal to noise ratio for further analyses.

Antibody dependent complement deposition (ADCD)

The ADCD assay was performed as described with modifications (Fischinger et al., 2019). Carboxylated microspheres (Luminex) were coupled with SARS-CoV-2 RBD protein (Bates et al., 2021c) (NR-52309 BEI Resources) by covalent NHS-ester linkages via EDC (1-Ethyl-3-[3-dimethylaminopropyl]carbodiimide hydrochloride, Thermo Scientific Pierce) and Sulfo-NHS (N-hydroxysulfosuccinimide, Thermo Scientific) per manufacturer instructions. A mixture of influenza antigens from strains H1N1 (NR-20083 and NR-51702, BEI Resources), H5N1 (NR-12148, BEI Resources), H3N2, B Yamagata lineage, and B Victoria lineage (NR-51702, BEI Resources) was used as a control. Serum samples were heated at 56°C for 30min. Antigen-coated microspheres (1250 per well) were added to a 96-well Bioplex Pro Flat Bottom plates (Bio-Rad) and incubated with serial dilutions of sera (1:10, 1:50 and 1:250) at 4°C for 16hrs. Freshly resuspended lyophilized guinea pig complement (Cedarlane) diluted 1:60 was added to the plate for 20min at 37°C. After washing off excess complement three times with15mM EDTA, anti-C3 PE-conjugated goat polyclonal IgG (MP Biomedicals) was added. The beads were then washed and C3 deposition quantified on a MAGPIX instrument containing xPONENT4.2 software (Luminex). The background signal, defined as MFI of microspheres incubated with PBS, was subtracted. Representative data from one dilution was chosen by the highest signal to noise ratio for further analyses.

Antibody dependent NK cell activation (ADNKA)

ADNKA assay was performed as described with modifications (Gunn et al., 2020). ELISA plates were coated with recombinant RBD antigen (300 ng/well) (Bates et al., 2021c) (BEI Resources NR-52309). Wells were washed, blocked, and incubated with serial dilutions of sera (1:10, 1:30, 1:90) for 2hrs at 37°C prior to adding CD16a.NK-92 cells (PTA-6967, ATCC) (5×10^4 cells/well) for 5hrs with brefeldin A (Biolegend), Golgi Stop (BD Biosciences) and anti-CD107a (clone H4A3, BD Biosciences). Cells were stained with anti-CD56 (clone 5.1H11, BD Biosciences) and anti-CD16 (clone 3G8, BD Biosciences) and fixed with 4% PFA. Intracellular cytokine staining to detect IFNγ (clone B27, BD Biosciences) and TNFα (clone Mab11, BD Biosciences) was performed in permeabilization buffer (Biolegend). Markers were measured using a BD LSRFortessa and analyzed by FlowJo10. CD16 expression was confirmed in all cells. NK cell degranulation and activation were calculated as percent of CD56+NK cells positive for CD107a, or IFNγ or TNFα expression. Representative data from one dilution was chosen by the highest signal to noise ratio for further analyses.

QUANTIFICATION AND STATISTICAL ANALYSIS

Statistical analysis and graphing were performed using Stata17 and GraphPad Prism9.0. Data are summarized using the descriptive measures median, minimum, maximum and percent (%). Wilcoxon matched pair signed rank tests were used to compare neutralization of live SARS-CoV-2 variants (Figure 1B) and glycoforms between antigen non-specific and RBD specific IgG (Figures 3C–3F, S3D, and S3E). Mann-U-Whitney tests were used to compare the neutralization of live SARS-CoV-2 variants between male and female (Figure S1C). Spearman rank correlations were used to examine bivariate associations between variables (Figures 2 and 5E, S1D and S2). Simple linear regression was used to examine the relationship between IgG glycoforms as the independent and Fc functional profiles as the dependent variables (Figures 3H–3K and S4). Multiple robust regression models were used to adjust for the effect of age and sex when comparing the study variables between individuals (Figures 1A, 1C–1H, 4, and S5). Z scores of each individual Fc feature was calculated and then summed to generate the cumulative Fc functional magnitude (Figures 5A and S6B). For

the radar plots (Figure 4I), Z scores of each individual RBD specific IgG glycoforms relative to bulk non-antigen specific IgG glycoforms were calculated and the median values for each age group were plotted. For the radar plots (Figure 5D), Z scores of each feature for each individual were calculated and the median values for each group were plotted. All p values are two-sided, and $p < 0.05$ was considered significant. In figures, asterisks denote statistical significance (*$p \leq 0.05$; **$p \leq 0.01$; ***$p \leq 0.001$; ***$p \leq 0.0001$) with comparisons specified by connecting lines.